induced NLRP3 and pro-IL-1β expression, but mature IL-1β was observed only after ATP treatment. These observations were confirmed with the monocyte cell line J774A.1 (Supplementary Figure S1a).

In order to express NLRP3 without the possible influence arising from a first signal, we established a method for artificial induction of NLRP3 with the Tet-on system. Transfection of an expression vector coding pro-IL-1β into MC/9 cells induced the expression of pro-IL-1β without expressing NLRP3 (Figure 1a, right panels), and doxycycline treatment induced the expression of wild type (WT)-NLRP3 that was tagged with EGFP (WT-NLRP3-Tet-on-MC/9). The expression of both pro-IL-1β and WT-NLRP3 were insufficient to release mature IL-1β and further ATP stimulation was necessary. These data indicated that the artificial gene induction system obviated the need for LPS as a first signal.

Following NLRP3 induction and ATP stimulation, we observed the release of high-mobility group box 1 (HMGB1), as well as mature IL-1β (Figure 1a). HMGB1 is a strong proinflammatory factor and normally maintained within the nucleus but released from cells undergoing necrosis.[17] Those results suggested that NLRP3 activation accompanied with mature IL-1β release could lead to necrotic cell death. However, we noted that even without expression of pro-IL-1β or cleavage of mature IL-1β, WT-NLRP3 induction and subsequent ATP stimulation induced HMGB1 (Figure 1b) and LDH release (Supplementary Figure S1b). This indicated that mature IL-1β was not required for NLRP3-mediated necrotic cell death.

Microscopic observation revealed that doxycycline treatment induced EGFP expression, indicating the induction of NLRP3 in the cytoplasm of WT-NLRP3-Tet-on-MC/9 cells (Supplementary Figure S1c). ATP stimulation induced an EGFP speckling in the cytoplasm (Supplementary Figure S1c). When WT-NLRP3-Tet-on-MC/9 cells co-expressed mCherry-tagged ASC, we observed red fluorescence, indicating that ASC was widely distributed in the cell (Figure 1c). ATP stimulation induced speckle formation of both ASC and NLRP3, and these speckles were co-localized (Figure 1c). These experiments were performed without pro-IL-1β expression, suggesting formation of the NLRP3-inflammasome even in the absence of pro-IL-1β. Cell swelling (Figure 1c) followed by membrane rupture was observed after ASC speckle formation.

Induction of CAPS-associated NLRP3 mutants was sufficient for cell death. Even though ATP stimulation alone did not induce HMGB1 release (Supplementary Figure S2a), ATP is known to induce cell damage.[15,16] Thus, we used CAPS-associated, spontaneously active NLRP3 mutants[18] to avoid ATP-induced cell damage, enabling us to examine whether or not the necrotic cell death observed was the consequence of inflammasome formation. The induction of mouse NLRP3 mutants (R258W, D301N and Y570C), corresponding to the major human CAPS-associated-mutations (R260W, D303N and Y570C, respectively),[19] by the Tet-on system in the presence of pro-IL-1β resulted in the release of mature IL-1β (Figure 2a and Supplementary Figure S2b) and caspase-1 activation (Figure 2b) even without a second signal after doxycycline treatment.

Unlike WT-NLRP3, expression of mutant NLRP3 in the Tet-on system showed HMGB1 release in the absence of ATP stimulation (Figure 2a and Supplementary Figure S2b), indicating that HMGB1 release was not the consequence of ATP stimulation but that of activated NLRP3 expression. HMGB1 release was also observed in the absence of pro-IL-1β without ATP stimulation (Supplementary Figure S2b). This indicates that pro-IL-1β was necessary for mature IL-1β release but not for NLRP3-related cell death. The same results were obtained from macrophage cell line J774A.1. The induction of CAPS-associated NLRP3 mutants produced mature IL-1β without a second signal (Supplementary Figure S2c) and resulted in HMGB1 release even without IL-1β cleavage (Supplementary Figure S2d).

Cell death induced by CAPS-associated NLRP3 mutants was necrotic. Microscope observation of NLRP3-Tet-on-MC/9 cells showed that mutant NLRP3 expression induced rapid cell swelling, cell membrane rupture and release of cell contents outside the cells (Figure 2c). Rapid swelling and membrane rupture were also observed in mutant NLRP3-Tet-on-J774A.1 cells (Supplementary Figure S2e), indicating that cell death with necrotic features was not specific to MC/9 cells. Electron microscopy revealed loss of the nuclear membrane cavity and fusion of chromatin with the cytosol, as well as obscured structures of cytosolic organelles in mutant NLRP3-expressing cells (Figure 2d).

The increases of EGFP intensity (an indicator of the level of EGFP-tagged NLRP3 expression) were similar between WT and D301N-NLRP3-Tet-on-MC/9 cells for the first 3 h after doxycycline treatment (Figures 2a and e and Supplementary Figure S3a). Cells expressing WT-NLRP3 continued the increase in EGFP intensities (Figures 2a and e and Supplementary Figure S3a), whereas cells expressing D301N stopped the increase of EGFP intensities after 6–24 h and became 7-amino-actinomycin (7-AAD) positive (Figures 2a and e and Supplementary Figure S3a). Fluorescent dyes such as 7-AAD and TOTO-3 iodide (TOTO-3) penetrate dead or damaged cells and label DNA. Together with annexin-V (which bears a high affinity for the phosphatidylserine that is externalized in early stages of apoptosis), 7-AAD can identify cell status. By expressing the CAPS-associated mutant NLRP3 (D301N), the annexin-V-/7-AAD-double negative viable MC/9 cells shifted directly to annexin-V-/7-AAD-double positive. This transition was similar to nigericin-treated necrotic cells that did not pass through an annexin-V-positive/7-AAD-negative apoptotic stage (Figure 2f and Supplementary Figure S3b), whereas cells expressing WT-NLRP3 remained viable. This result indicates that necrotic cell death was induced following the expression of mutant NLRP3.

Note further that none of the cells expressing mutant NLRP3 showed cleavage of either caspase-3 or PARP, both of which were observed in apoptotic cells treated with actinomycin D (Figure 2g). This observation also indicated that NLRP3-mediated cell death was not apoptotic. The same results were obtained in J774A.1 cells (Supplementary Figure S3c).

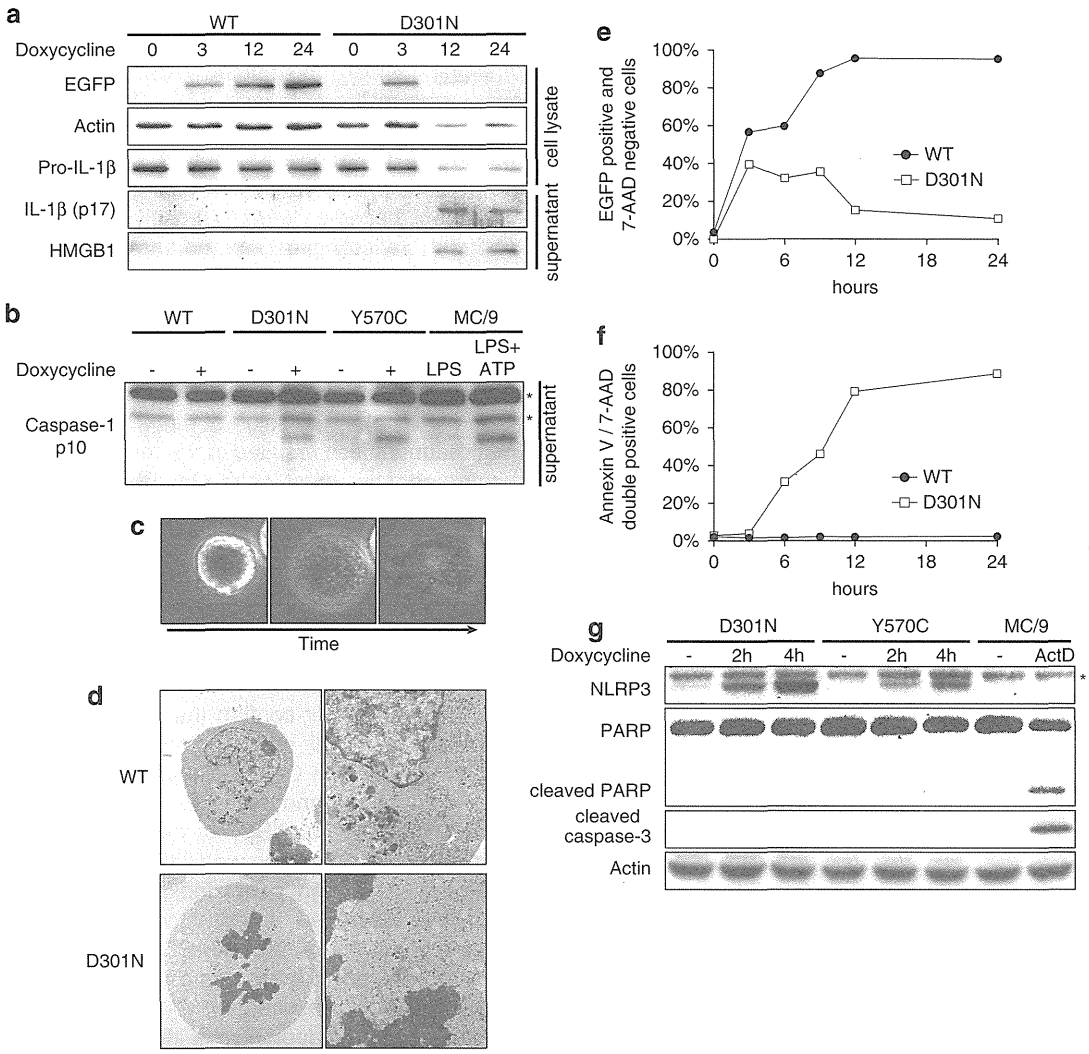

Figure 2 CAPS-associated mutant NLRP3-induced necrotic cell death in the absence of pro-IL-1β. (**a**) WT and D301N-NLRP3-Tet-on-MC/9 cells were transfected with the pro-IL-1β-pMX-IP retroviral vector and incubated for 48 h. NLRP3-Tet-on-MC/9 cells (1×10^6) were treated with 1 μg/ml doxycycline. Cells and supernatants were harvested for western blotting at the indicated time points after doxycycline treatment. (**b**) WT, D301N and Y570C-NLRP3-Tet-on-MC/9 cells (1×10^6) were stimulated with 1 μg/ml doxycycline for 16 h. MC/9 cells were pretreated with 0.5 μg/ml LPS for 2 h and stimulated with 5 mM ATP for 45 min. The supernatants were harvested for immunoblotting of caspase-1. The indicate non-specific band. (**c**) Confocal scanning image of cell death caused by the expression of CAPS-associated mutant NLRP3, taken 6 h after doxycycline treatment. Scanning was performed at 1-min intervals with an Olympus FV10i. (**d**) Upper panels: electron microscopy of WT-NLRP3-Tet-on-MC/9 cells 10 h after doxycycline treatment. Lower panels: electron microscopy of D301N-NLRP3-Tet-on-MC/9 cells 10 h after doxycycline treatment. (**e** and **f**) WT and D301N-NLRP3-Tet-on-MC/9 cells were treated with 1 μg/ml doxycycline, and the signal intensities of EGFP and Alexa647-annexin-V/ 7-AAD staining were analyzed by flow cytometry. MC/9 cells were incubated with 20 μg/ml nigericin for 6 h as a necrosis control. (**g**) CAPS-associated mutant NLRP3-Tet-on-MC/9 cells (1×10^6) were treated with 1 μg/ml doxycycline for the indicated time and the cells were harvested for immunoblotting of NLRP3, PARP, cleaved caspase-3 and actin. The asterisk indicates non-specific band. MC/9 cells were incubated with 100 nM actinomycin D for 8 h as an apoptosis control

Loss of viability mediated by CAPS-associated NLRP3 mutants was programmed cell death. In contrast to accidental cell death, programmed cell death is inhibited when its signaling pathways are blocked. Thus, we examined if necrotic cell death induced by mutant NLRP3 could be blocked with inhibitors. We previously reported that cell death induced by LPS treatment of monocytes isolated from CAPS patients was blocked by cathepsin B inhibitor CA074-Me,[7] and that the cell death induced by transient expression of CAPS-associated mutant NLRP3 was blocked by CA074-Me and caspase inhibitors.[9] The cell death caused by CAPS-associated NLRP3 mutants in the Tet-on system (Figure 3a) was attenuated by both CA074-Me and pan-caspase inhibitor Z-VAD-fmk (Figure 3a). These data indicate that loss of viability was the result of programmed cell death with no requirements for LPS treatment or exogenous DNA transfection.

Specific caspase inhibitors, however, did not block cell death (Figure 3b) nor did simultaneous addition of multiple specific caspase inhibitors (data not shown). These results suggest that loss of viability was not dependent on caspase activities. The other pan-caspase inhibitors, Boc-D-fmk, ac-VAD-cho and Q-VD-OPh also failed to block cell death even at higher concentrations (Figure 3c

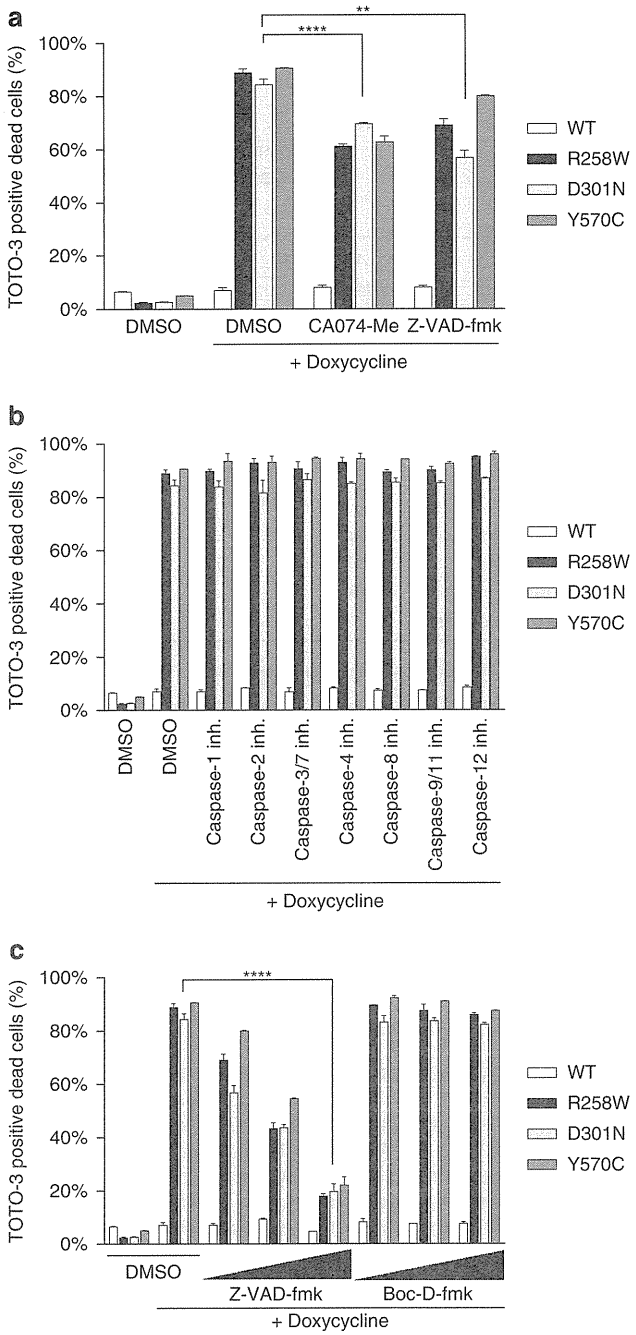

Figure 3 Cell death induced by CAPS-associated NLRP3 mutants was programmed cell death. (**a** and **b**) WT and mutant NLRP3-Tet-On-MC/9 cells were treated with 1 μg/ml doxycycline for 12 h in addition to cathepsin B inhibitor CA074-Me (20 μM), pan-caspase inhibitor Z-VAD-fmk (10 μM), caspase-1 inhibitor Z-YVAD-cho (10 μM), caspase-2 inhibitor, Z-VDVAD-fmk (10 μM), caspase-3/7 inhibitor Z-DEVD-fmk (10 μM), caspase-4 inhibitor Z-LEVD-fmk (10 μM), caspase-8 inhibitor Z-IETD-fmk (10 μM), caspase-9/11 inhibitor Z-LEHD-fmk (10 μM) or caspase-12 inhibitor Z-ATAD-fmk (10 μM). Cells were stained with 100 nM TOTO-3 for 5 min and analyzed by flow cytometry. (**c**) WT and mutant NLRP3-Tet-on-MC/9 cells were treated with 1 μg/ml doxycycline for 12 h in addition to pan-caspase inhibitor Z-VAD-fmk or Boc-D-fmk (10/20/40 μM). **, $P<0.01$; and ****, $P<0.0001$

and Supplementary Figure S4a-b). The results suggest that Z-VAD-fmk inhibited cell death presumably due to its 'off-target' effects.

Z-VAD-fmk and CA074-Me inhibited necrotic cell death at different steps. Without doxycycline treatment, we observed widely distributed ASC in the cells stably expressing mCherry-tagged ASC. Those cells were unsusceptible to Yo-Pro-1 staining. However, when we expressed CAPS-associated mutant NLRP3 by doxycycline, the diffused presence of ASC changed to a speckle pattern and then became 'green' (positive) when stained with Yo-Pro-1, reflecting cell membrane damage (Supplementary Figure S4c).

After mutant NLRP3 expression by doxycycline under DMSO treatment as vehicle, most cells converted the distribution pattern of ASC to speckle pattern and became positive for Yo-Pro-1 (Figure 4a, upper and middle left panels, and Figure 4b). Expression of mutant NLRP3 under Z-VAD-fmk treatment also resulted in the formation of ASC speckle, but importantly, most cells stayed negative for Yo-Pro-1 (Figure 4a, middle right panel, and Figure 4b), indicating that those cells could avoid the cell death even after ASC speckle formation. In contrast, when treated with CA074-Me, most cells retained the diffused appearance of ASC and negative for Yo-Pro-1 (Figure 4a, lower left panel, and Figure 4b), suggesting that CA074-Me inhibited the cell death before ASC oligomerization step.

In order to further confirm the processes those inhibitors blocked in the cell death pathway, we treated the cells simultaneously with CA074-Me and Z-VAD-fmk (Figure 4a, lower right panel), and observed that most cells showed the diffused presence of ASC, as did CA074-Me-treated cells. Moreover, some cells escaped cell death with ASC speckling (Figure 4a, lower right panel, indicated by arrows), leading to an overall decrease of dead cells in number compared with the condition treated with CA074-Me alone (Figure 4b). This result indicated that some cells that were not blocked by CA074-Me were rescued by Z-VAD-fmk even after ASC oligomerization, supporting the idea that CA074-Me worked on a step prior to both of ASC oligomerization and the process that was susceptible to Z-VAD-fmk.

ASC was required in NLRP3-induced necrotic cell death, whereas caspase-1 was not. In order to investigate whether ASC oligomerization was only an accessory event or a critical process for programmed cell death, we knocked down ASC in NLRP3-Tet-on-MC/9 cells. This led to decreases of both HMGB1 release and TOTO-3-positive dead cells upon expression of D301N and Y570C (Figures 5a and b), even though NLRP3 was expressed at similar levels in scrambled-small hairpin RNA (shRNA)- and *Asc*-shRNA-expressing NLRP3-Tet-on-MC/9 cells (Figure 5a). Thus, cell death induced by NLRP3 activation required ASC.

The caspase-1 inhibitor did not block NLRP3-induced cell death (Figure 3b). That result indicated that the activity of caspase-1 was not required for the cell death. We further investigated the possible requirement for caspase-1 in cell death by using shRNA that targeted caspase-1. Knocking down caspase-1 did not block cell death induced by expressing CAPS-associated mutant NLRP3 (Figures 5c and d). These results likely indicate that caspase-1 was not involved in cell death and support the previous report that macrophages derived from caspase-1 knockout mice also

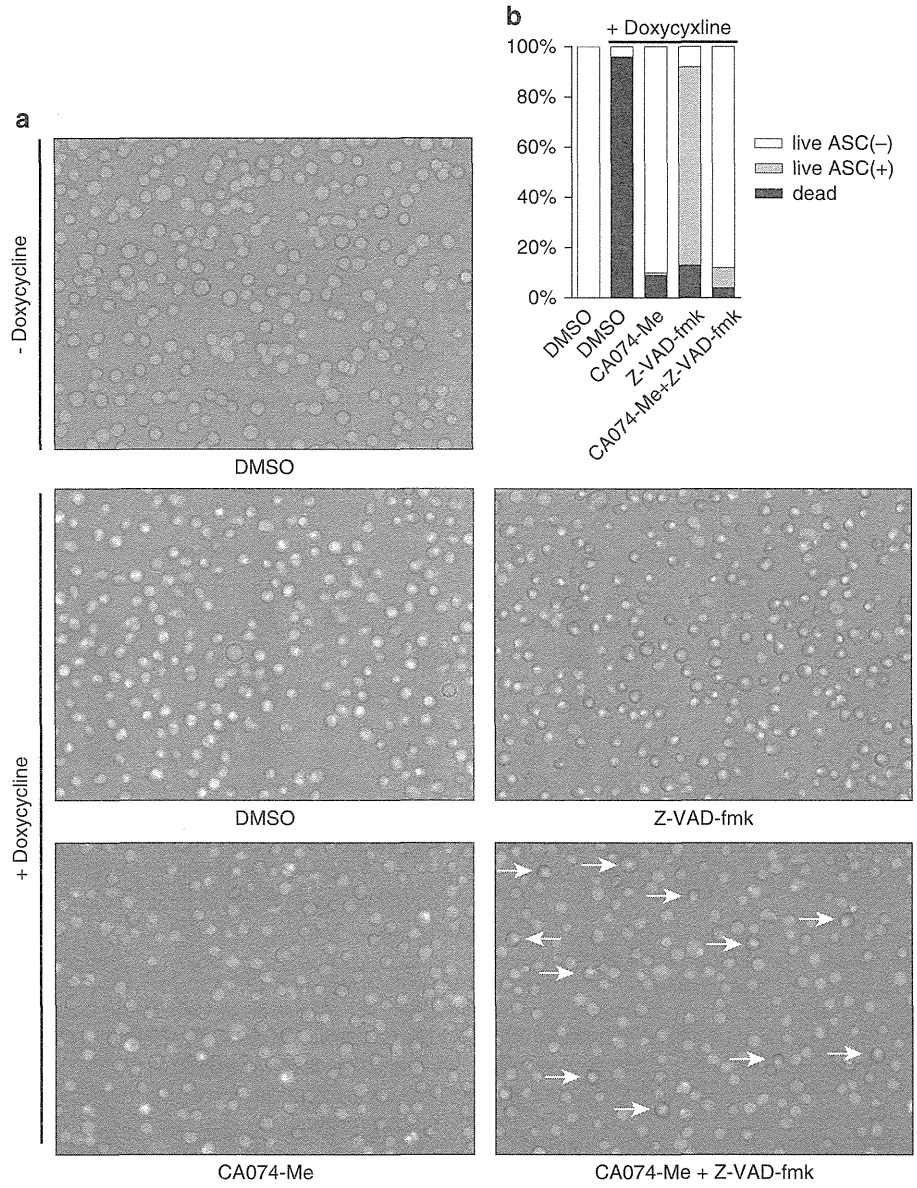

Figure 4 Z-VAD-fmk and CA074-Me inhibited necrotic cell death at different steps. (**a** and **b**) D301N-NLRP3-Tet-on-MC/9 cells stably expressing ASC-mCherry-pMX-IN were treated with 1 μg/ml doxycycline for 12 h in addition to 50 μM CA074-Me or 50 μM Z-VAD-fmk. Cells were stained with 0.1 μM Yo-Pro-1 for 5 min and cell morphologies were examined under a fluorescent microscope. The number of cells containing ASC speckling among Yo-Pro-1 negative live cells was counted; enumeration included over 100 cells based on pictures taken with a Carl ZEISS Axio Observer D1 for three independent trials

showed NLRP3/ASC-dependent cell death and exacerbated the inflammatory response induced by *Shigella flexneri*.[6]

NLRP3-mediated necrotic cell death resulted in a neutrophilic inflammatory response without IL-1β. CAPS patients are known to have neutrophil-rich urticarial rashes.[20] In order to investigate if the necrotic cell death caused by activated NLRP3 induced a neutrophilic inflammatory response, we performed neutrophil infiltration assays using an air-pouch model. NLRP3-Tet-on-MC/9 cells were injected and incubated in the air-pouch and all the cells in the pouch were collected for flow cytometric analysis. WT-NLRP3-Tet-on-MC/9 cells increased the level of NLRP3 expression upon doxycycline administration (Supplementary Figure S5a, middle panels). Importantly, the injected WT-NLRP3-Tet-on-MC/9 cells retained viability even after doxycycline administration (Supplementary Figure S5a, upper panels, and Supplementary Figure S5b). In contrast, mutant NLRP3-Tet-on-MC/9 cells disappeared after doxycycline administration, presumably due to necrotic cell death (Supplementary Figure S5a, upper panels, and Supplementary Figure S5b).

Pretreatment with LPS induces the expression of pro-IL-1β. Consequently, mature IL-1β is secreted from LPS-pretreated cells when expressing CAPS-associated mutant NLRP3. Mature IL-1β secretion combined with necrotic cell death in

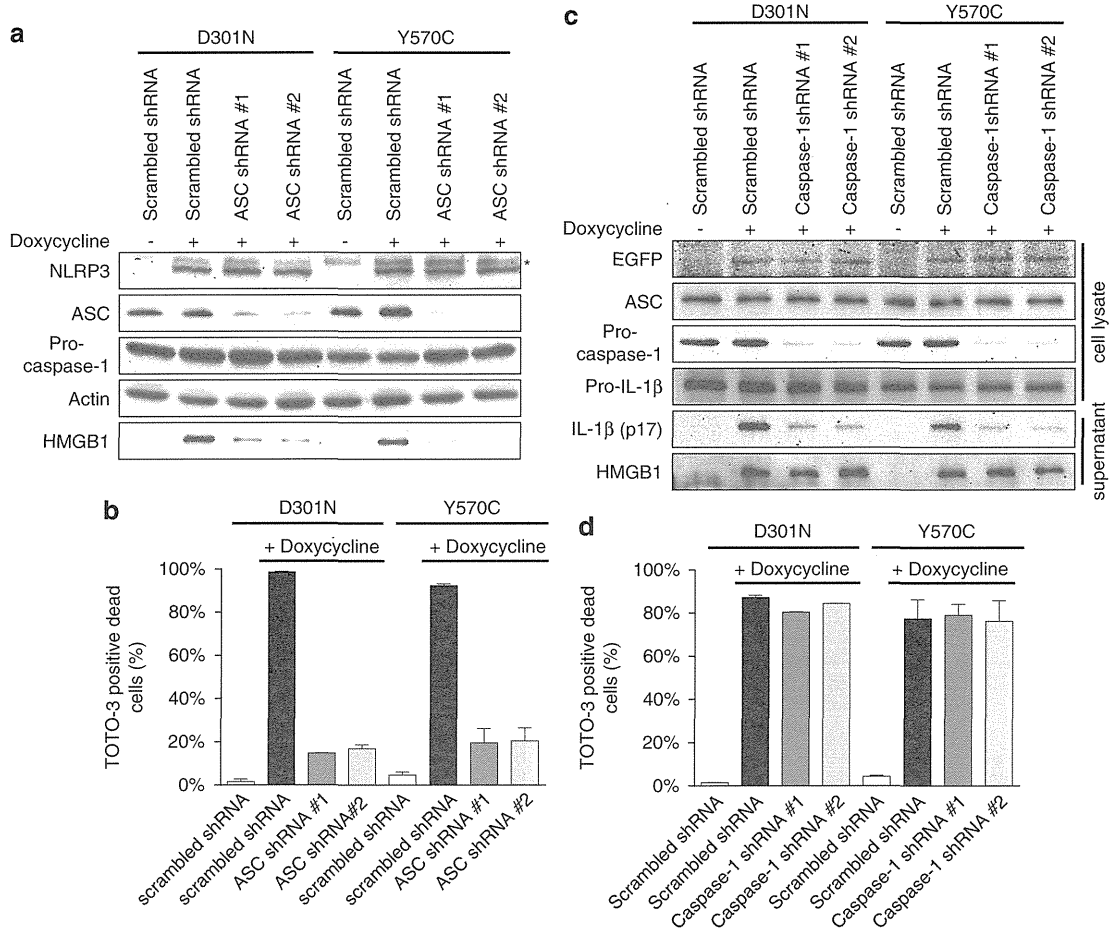

Figure 5 ASC was required for necrotic cell death induced by CAPS-associated mutant NLRP3, whereas caspase-1 was not. (**a**) D301N and Y570C-NLRP3-Tet-on-MC/9 cells were transduced with scrambled or *Asc*-targeting shRNA lentiviral vector and selected by puromycin for 1 week. Cells (1×10^6) in 1 ml of medium were treated with 1 μg/ml doxycycline. Cells were collected 3 h later while supernatants were harvested 24 h after doxycycline treatment. Immunoblotting of NLRP3, ASC, caspase-1, actin and HMGB1 was performed on the cells or the supernatant. The asterisk indicates non-specific band. (**b**) D301N and Y570C-NLRP3-Tet-on-MC/9 cells transduced with scrambled or *Asc*-targeting shRNA lentiviral vector were treated with 1 μg/ml doxycycline for 12 h. Cells were stained with 100 nM TOTO-3 for 5 min, and TOTO-3-positive dead cells were counted by flow cytometry. (**c**) D301N and Y570C-NLRP3-Tet-on-MC/9 cells were transduced with scrambled or *Casp1*-targeting shRNA lentiviral vector and selected by puromycin for 1 week. Cells were transfected with the pro-IL-1β-pMX-IP retroviral vector and incubated for 48 h. Cells (1×10^6) in 1 ml of medium were treated with 1 μg/ml doxycycline. Cells were collected 3 h later while supernatants were harvested 12 h after doxycycline treatment. Immunoblotting of EGFP, ASC, caspase-1, IL-1β and HMGB1 was performed on the cells or the supernatant. (**d**) D301N or Y570C-NLRP3-Tet-on-MC/9 cells (in which caspase-1 was knocked down) were treated with 1 μg/ml doxycycline for 12 h. Cells were stained with 100 nM TOTO-3 for 5 min, and TOTO-3-positive dead cells were counted by flow cytometry

the air-pouch resulted in neutrophil infiltration (Figures 6a and b and Supplementary Figure S5a, lower panels). In contrast, neutrophils did not increase in the air-pouch injected with WT-NLRP3-Tet-on-MC/9 cells, unaccompanied by IL-1β release (Figure 6b). Necrotic cell death without IL-1β secretion (which can be achieved in this system by administering doxycycline without LPS pretreatment) also induced neutrophil infiltration, though fewer in number relative to that induced by necrotic cell death with IL-1β (Figure 6a). Such data indicate that necrotic cell death in itself can cause and exacerbate the neutrophilic inflammatory response.

Discussion

In this study, we showed that expression of CAPS-associated mutant NLRP3 itself induced programmed necrotic cell death independently of IL-1β processing and that cell death induced by activated NLRP3 exacerbated the inflammatory response in addition to IL-1β. We clarified the mechanism of NLRP3-mediated cell death by using a CAPS-associated mutant NLRP3, thereby avoiding exposure to a pathogen, LPS stimulation or cell damage caused by second signals. Our study further supports previous data showing that transient expression of CAPS-associated mutant NLRP3-induced necrotic cell death,[9] and that LPS, accompanied with mutant NLRP3 expression, induced necrotic cell death in monocytes isolated from CAPS patients.[6–8]

The characteristic programmed necrosis regulated by NLRP3 has been termed pyronecrosis.[6] In pyronecrosis, cell lysis and HMGB1 release occurred after ASC speckle formation and cell death was inhibited by Z-VAD-fmk. This report led us to compare pyronecrosis and pyroptosis,

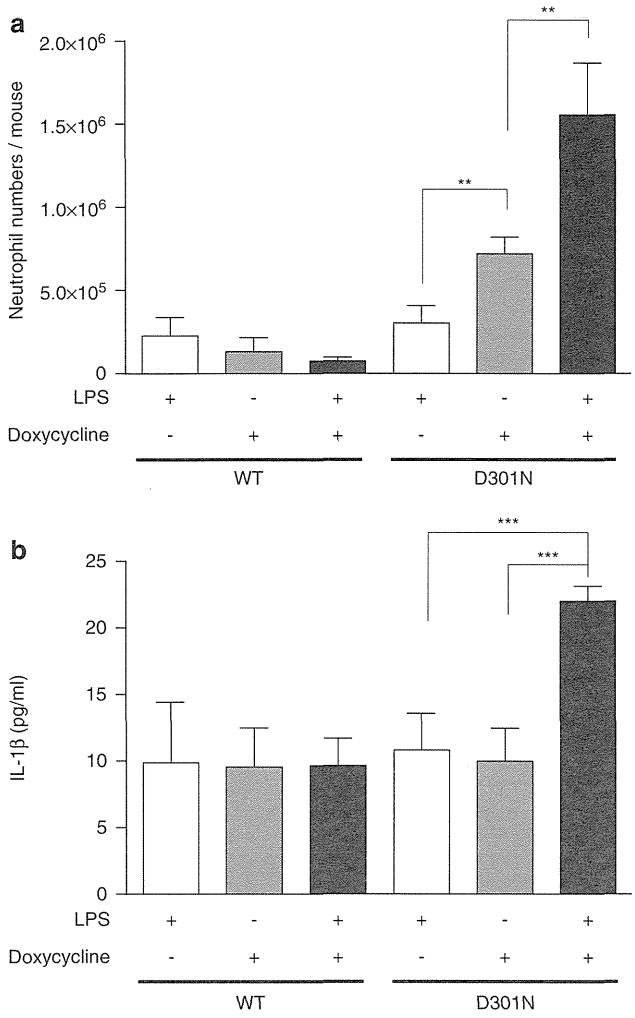

Figure 6 Necrotic cell death recruited neutrophils without IL-1β. (**a**) WT or D301N-NLRP3-Tet-on-MC/9 cells (1×10^7) pretreated with 0.5 μg/ml LPS for 2 h were injected into an air-pouch located on the backs of mice. Some mice were given doxycycline-containing drinking water 24 h before cell injection. After 16 h, the cells in the pouch were harvested by injecting 1 ml PBS and stained with Alexa647-Gr-1 and PE-F4/80 antibodies for flow cytometric analysis. Cells located in the gate A (Supplementary Fig. S5a), other than MC/9 (gate B) or dead cells, were analyzed for Alexa647-Gr-1 and PE-F4/80 axes. (**b**) WT or D301N-NLRP3-Tet-on-MC/9 cells (1×10^7), pretreated with 0.5 μg/ml LPS for 2 h, were injected into an air-pouch. Some mice were given doxycycline-containing drinking water 24 h before cell injection. After 8 h, the lavage fluid in the air-pouch was harvested by injecting 300 μl PBS and IL-1β ELISA was performed. All results are representative of at least three separate experiments ($n=5$ mice per condition). **, $P<0.01$; and ***, $P<0.001$

the latter being caspase-1-dependent programmed necrosis in response to intracellular bacteria such as *Salmonella*.[21,22] Pyroptosis requires caspase-1 activity and is inhibited by caspase-1 inhibitor or pan-caspase inhibitor Z-VAD-fmk.[23–25] Our data, however, demonstrated that a caspase-1 inhibitor did not inhibit pyronecrosis, cell death caused by CAPS-associated mutant NLRP3 expression. Moreover, knocking down caspase-1 in our study did not prevent cell death, supporting the previous reports that macrophages derived from caspase-1 knockout mice also showed NLRP3-mediated pyronecrosis induced by *Shigella*.[6]

Most pathogens induce not only NLRP3 but also pro-IL-1β expression. Therefore, the effect of NLRP3-mediated pyronecrosis is the combined outcome of cell death and IL-1β. Here, we first time show that NLRP3-mediated pyronecrosis recruits neutrophils even in the absence of IL-1β and it may contribute to the clearance of pathogens. The result that NLRP3-mediated cell death might possess the ability to evoke inflammation even in the absence of IL-1β is reasonable, and hence pyronecrosis does not require the activity of caspase-1 that cleaves IL-1β to its mature form.

Cathepsin B is a cysteine protease that is normally located in lysosomes and degrades various proteins in an acidic environment.[26] Cathepsin B can be lethal if released from the lysosomal compartment. Cathepsin B inhibitor CA074-Me abrogated NLRP3-dependent pyronecrois so that several groups, including us, deduced that cathepsin B was involved in pyronecrosis after inflammasome formation.[9,27] However, if CA074-Me could inhibit the cell death at the step after inflammasome formation, the rescued live cells by CA074-Me must bear ASC speckle, which was not occurred in our experiment. This observation may suggest that the hypothesis that cathepsin B is involved in pyronecrosis after inflammasome formation is incorrect, and that cathepsin B has some role in the process prior to inflammasome formation. This idea is also supported from the finding that pyroptosis, which is ASC-mediated cell death, was not blocked by cathepsin B inhibitor.[28]

Cathepsin B released from ruptured lysosomes after phagocytosis of large particles such as silica or β-amyloid is thought to cleave an unidentified substrate and trigger activation of the inflammasome.[29,30] However, when cells expressed the CAPS-associated mutant NLRP3 with the Tet-on system, a cathepsin B inhibitor blocked both cell death and mature IL-1β release (Supplementary Figure S5c), even though a formation of large particles and lysosomal rupture was not involved (data not shown). Consider also that LPS-induced death of human monocytes carrying the NLRP3 mutation (which cannot phagocytize large particles) was also blocked by a cathepsin B inhibitor.[7] As CA074-Me inhibited NLRP3-mediated cell death even without a formation of large particles and lysosomal rupture, careful attention should be paid to the deduced involvement of cathepsin B in inflammasome formation. Thus, the theory might require re-evaluation that phagocytosis of large particles induces lysosome rupture and cytosolic activation of cathepsin B, resulting in NLRP3 activation. Additional information regarding how inhibitors such as CA074-Me and Z-VAD-fmk suppress cell death might provide clues, clarifying the mechanism of inflammasome activation and NLRP3-mediated necrotic programmed cell death.

In this study, we demonstrated that expression of CAPS-associated mutant NLRP3 itself induced programmed necrotic cell death downstream of ASC oligomerization, independent of IL-1β processing. This type of cell death may have wide significance in immune responses because it is mediated by NLRP3, a protein that senses not only pathogens but also danger-associated signals, and presumably contributes to neutrophil infiltration in urticarial rashes in CAPS or other diseases such as gout in which NLRP3 is proposed to contribute to the pathogenesis.

Materials and Methods

Plasmids. The expression plasmids for mouse NLRP3-EGFP, its CAPS-associated-mutants (namely R258W, D301N and Y570C) and ASC were described previously.[19] In order to establish the Tet-on system, NLRP3-EGFP and its mutants were inserted into pRetroX-Tight-Pur or pRetroX-Tight-Hyg retrovirus vectors (Clontech, Mountain View, CA, USA). The following primers were used to amplify the pro-IL-1β transcript: forward primer, 5′-GCGCTCGAGGC AGCTATGGCAACTGTTCCTG-3′, and reverse primer, 5′-CGCGCGGCCGCTTA GGAAGACACGGATTCCATGG-3′. ASC was fused with mCherry fluorescent protein (Clontech). The pro-IL-1β transcript and ASC-mCherry were cloned into pMX-IRES-puro (pMX-IP) vector (provided by Dr. T Kitamura, University of Tokyo, Tokyo, Japan) or pMX-IRES-human nerve growth factor receptor p75 (pMX-IN) vector (provided by Drs. A Onodera and T Nakayama, Chiba University, Chiba, Japan).

Generation of cell lines. Mouse mast cell line MC/9 cells and mouse monocyte cell line J774A.1 cells were maintained in DMEM medium with 10% FBS. In order to establish NLRP3-Tet-on-MC/9 and NLRP3-Tet-on-J774A.1 cells by the Tet-on system, viral transduction was performed as described previously.[19] MC/9 and J774A.1 cells were incubated with retroviral supernatants for 15 h with 4 μg/ml polybrene (Sigma-Aldrich, St Louis, MO, USA), and selected with G418 (3 mg/ml), puromycin (3 μg/ml) or hygromycin (50 μg/ml), depending on the selection markers. Cells transfected with expression vector containing human nerve growth factor receptor were enriched twice by MACS with anti-human NGFR (C40-1457; BD Pharmingen, San Jose, CA, USA).

Western blot Assays. Cells were washed in PBS and lysed in ice-cold lysis buffer M-PER (Thermo Fisher, Waltham, MA, USA) supplemented with protease inhibitor cocktails. Lysates and supernatants were centrifuged for 5 min and the supernatants were boiled for 5 min in sample buffer. After SDS-PAGE, immunoblots were processed using antibodies against EGFP (Clontech), NLRP3 (Cryo-2; AdipoGen, San Diego, CA, USA), ASC (a gift from Dr. J Masumoto, Shinshu University, Nagano, Japan), caspase-1 (sc-514; Santa Cruz, Dallas, TX, USA), IL-1β (AB-401; R&D Systems, Minneapolis, MN, USA), HMGB1 (14-9900; eBioscience, San Diego, CA, USA), actin (sc-8432; Santa Cruz), caspase-3 (9661; Cell Signaling, Danvers, MA, USA) or PARP (9542; Cell Signaling).

Reagents. The pan-caspase inhibitors Z-VAD-fmk (R&D Systems), ac-VAD-cho (MERCK, Whitehouse Station, NJ, USA), Q-VD-OPh and Boc-D-fmk (BioVision, Milpitas, CA, USA), and specific caspase inhibitors Z-YVAD-fmk (MERCK), Z-VDVAD-fmk, Z-LEVD-fmk and Z-ATAD-fmk (MBL, Nagoya, Japan), Z-YVAD-cho, Z-DEVD-fmk, Z-IETD-fmk and Z-LEHD-fmk (R&D Systems), Z-FA-fmk (BD Pharmingen) were purchased. Cathepsin B inhibitor CA074-Me was obtained from MERCK. Ultra pure LPS was from InvivoGen, San Diego, CA, USA. ATP was from Sigma-Aldrich. Doxycycline and Tet system-approved FBS were obtained from Clontech.

Flow cytometry. Expression levels of EGFP-tagged proteins were assessed by flow cytometry (Canto II, BD, Franklin Lakes, NJ, USA). Dead cells were analyzed using TOTO-3 (Invitrogen, San Diego, CA, USA) staining.

Apoptosis and necrosis assays. The mode of cell death, namely apoptosis or necrosis, was determined primarily by the morphology of the dying cells under microscopic observation. The proportions of apoptotic and necrotic cells were also determined by flow cytometry[9] after staining with Alexa 647-annexin-V (BioLegend, San Diego, CA, USA) and 7-AAD (BD Pharmingen).

ELISA assays. The amount of IL-1β was determined using an OptELISA kit (eBioscience), according to the manufacturer's protocol.

LDH assays. LDH activities in the culture supernatants were measured using a CytoTox 96 assay kit (Promega, Madison, WI, USA).

Electron microscopy. Cells were fixed in 2% glutaraldehyde in phosphate buffer. Routine procedures for observation by electron microscopy were performed by Filgen Inc (Nagoya, Japan).

Knockdown of ASC and caspase-1. ASC or caspase-1 expression was knocked down using shRNA inserted into a lentiviral pLKO.1 puro vector (Sigma-Aldrich). MC/9 cells stably expressing Tet-on inducible NLRP3 were exposed to *Asc*-targeting, *Casp1*-targeting or control shRNA lentivirus and selected by puromycin.

Fluorescent microscopy. Cells were observed with a Carl Zeiss Axio Observer microscope or Olympus FV10i. In some experiments, cells were stained with 0.1 μM Yo-Pro-1 (Invitrogen) for 5 min to distinguish necrotic dead cells from living cells.

Air-pouch model. The Chiba University Animal Care and Use Committee approved the animal procedures used in this study. Air pouches were established in 4-week-old male C57BL/6 mice by injecting 3 and 1.5 ml of sterile air at day 0 and day 3, respectively, under the dorsal skin of mice.[31] At day 5, mice were administered with 2 mg/ml doxycycline in drinking water. At day 6, NLRP3-Tet-on-MC/9 cells were pretreated with 0.5 μg/ml LPS for 2 h, washed with sterile PBS three times, incubated in culture medium for 4 h and washed three times with sterile PBS to eliminate the effect of tumor necrosis factor-α, mainly released 3 h after LPS stimulation (data not shown). After these pretreatments, mice were injected with 1×10^7 NLRP3-Tet-on-MC/9 cells in 1 ml PBS. At day 7, the pouches were washed with 1 ml of PBS and the lavage fluid and cells were harvested for ELISA and FACS analysis with PE-anti-mouse F4/80 and Alexa 647-anti-mouse Gr-1 (Ly-6G) antibodies from BioLegend.

Conflict of Interest

The authors declare no conflict of interest.

Acknowledgements. This work was supported in part by grant-in-aid from the MEXT and from the Ministry of Health, Labour and Welfare, Japan.

1. Tschopp J, Schroder K. NLRP3 inflammasome activation: The convergence of multiple signalling pathways on ROS production? *Nat Rev Immunol* 2010; **10**: 210–215.
2. Meylan E, Tschopp J, Karin M. Intracellular pattern recognition receptors in the host response. *Nature* 2006; **442**: 39–44.
3. Jones DA, Takemoto D. Plant innate immunity - direct and indirect recognition of general and specific pathogen-associated molecules. *Curr Opin Immunol* 2004; **16**: 48–62.
4. Chisholm ST, Coaker G, Day B, Staskawicz BJ. Host-microbe interactions: shaping the evolution of the plant immune response. *Cell* 2006; **124**: 803–814.
5. Hoffman HM, Mueller JL, Broide DH, Wanderer AA, Kolodner RD. Mutation of a new gene encoding a putative pyrin-like protein causes familial cold autoinflammatory syndrome and Muckle-Wells syndrome. *Nat Genet* 2001; **29**: 301–305.
6. Willingham SB, Bergstralh DT, O'Connor W, Morrison AC, Taxman DJ, Duncan JA *et al.* Microbial pathogen-induced necrotic cell death mediated by the inflammasome components CIAS1/cryopyrin/NLRP3 and ASC. *Cell Host Microbe* 2007; **2**: 147–159.
7. Saito M, Nishikomori R, Kambe N, Fujisawa A, Tanizaki H, Takeichi K *et al.* Disease-associated CIAS1 mutations induce monocyte death, revealing low-level mosaicism in mutation-negative cryopyrin-associated periodic syndrome patients. *Blood* 2008; **111**: 2132–2141.
8. Reddy S, Jia S, Geoffrey R, Lorier R, Suchi M, Broeckel U *et al.* An autoinflammatory disease due to homozygous deletion of the IL1RN locus. *N Engl J Med* 2009; **360**: 2438–2444.
9. Fujisawa A, Kambe N, Saito M, Nishikomori R, Tanizaki H, Kanazawa N *et al.* Disease-associated mutations in CIAS1 induce cathepsin B-dependent rapid cell death of human THP-1 monocytic cells. *Blood* 2007; **109**: 2903–2911.
10. Gilroy EM, Hein I, van der Hoorn R, Boevink PC, Venter E, McLellan H *et al.* Involvement of cathepsin B in the plant disease resistance hypersensitive response. *Plant J* 2007; **52**: 1–13.
11. Rathinam VA, Jiang Z, Waggoner SN, Sharma S, Cole LE, Waggoner L *et al.* The AIM2 inflammasome is essential for host defense against cytosolic bacteria and DNA viruses. *Nat Immunol* 2010; **11**: 395–402.
12. Fernandes-Alnemri T, Yu JW, Juliana C, Solorzano L, Kang S, Wu J *et al.* The AIM2 inflammasome is critical for innate immunity to Francisella tularensis. *Nat Immunol* 2010; **11**: 385–393.
13. Jones JW, Kayagaki N, Broz P, Henry T, Newton K, O'Rourke K *et al.* Absent in melanoma 2 is required for innate immune recognition of Francisella tularensis. *Proc Natl Acad Sci USA* 2010; **107**: 9771–9776.
14. Nakahira K, Haspel JA, Rathinam VA, Lee SJ, Dolinay T, Lam HC *et al.* Autophagy proteins regulate innate immune responses by inhibiting the release of mitochondrial DNA mediated by the NALP3 inflammasome. *Nat Immunol* 2011; **12**: 222–230.
15. Hanley PJ, Kronlage M, Kirschning C, del Rey A, Di Virgilio F, Leipziger J *et al.* Transient P2 $\times$ 7 receptor activation triggers macrophage death independent of Toll-like receptors 2 and 4, caspase-1, and pannexin-1 proteins. *J Biol Chem* 2012; **287**: 10650–10663.

16. Hentze H, Lin XY, Choi MS, Porter AG. Critical role for cathepsin B in mediating caspase-1-dependent interleukin-18 maturation and caspase-1-independent necrosis triggered by the microbial toxin nigericin. *Cell Death Differ* 2003; **10**: 956–968.
17. Scaffidi P, Misteli T, Bianchi ME. Release of chromatin protein HMGB1 by necrotic cells triggers inflammation. *Nature* 2002; **418**: 191–195.
18. Agostini L, Martinon F, Burns K, McDermott MF, Hawkins PN, Tschopp J. NALP3 forms an IL-1beta-processing inflammasome with increased activity in Muckle-Wells autoinflammatory disorder. *Immunity* 2004; **20**: 319–325.
19. Nakamura Y, Kambe N, Saito M, Nishikomori R, Kim YG, Murakami M *et al.* Mast cells mediate neutrophil recruitment and vascular leakage through the NLRP3 inflammasome in histamine-independent urticaria. *J Exp Med* 2009; **206**: 1037–1046.
20. Shinkai K, McCalmont TH, Leslie KS. Cryopyrin-associated periodic syndromes and autoinflammation. *Clin Exp Dermatol* 2008; **33**: 1–9.
21. Fernandes-Alnemri T, Wu J, Yu JW, Datta P, Miller B, Jankowski W *et al.* The pyroptosome: a supramolecular assembly of ASC dimers mediating inflammatory cell death via caspase-1 activation. *Cell Death Differ* 2007; **14**: 1590–1604.
22. Monack DM, Detweiler CS, Falkow S. Salmonella pathogenicity island 2-dependent macrophage death is mediated in part by the host cysteine protease caspase-1. *Cell Microbiol* 2001; **3**: 825–837.
23. Brennan MA, Cookson BT. Salmonella induces macrophage death by caspase-1-dependent necrosis. *Mol Microbiol* 2000; **38**: 31–40.
24. Bergsbaken T, Cookson BT. Macrophage activation redirects yersinia-infected host cell death from apoptosis to caspase-1-dependent pyroptosis. *PLoS Pathog* 2007; **3**: e161.
25. Reisetter AC, Stebounova LV, Baltrusaitis J, Powers L, Gupta A, Grassian VH *et al.* Induction of inflammasome-dependent pyroptosis by carbon black nanoparticles. *J Biol Chem* 2011; **286**: 21844–21852.
26. Turk V, Stoka V, Vasiljeva O, Renko M, Sun T, Turk B *et al.* Cysteine cathepsins: from structure, function and regulation to new frontiers. *Biochim Biophys Acta* 2012; **1824**: 68–88.
27. Duncan JA, Gao X, Huang MT, O'Connor BP, Thomas CE, Willingham SB *et al.* Neisseria gonorrhoeae activates the proteinase cathepsin B to mediate the signaling activities of the NLRP3 and ASC-containing inflammasome. *J Immunol* 2009; **182**: 6460–6469.
28. Lamkanfi M, Sarkar A, Vande Walle L, Vitari AC, Amer AO, Wewers MD *et al.* Inflammasome-dependent release of the alarmin HMGB1 in endotoxemia. *J Immunol* 2010; **185**: 4385–4392.
29. Hornung V, Bauernfeind F, Halle A, Samstad EO, Kono H, Rock KL *et al.* Silica crystals and aluminum salts activate the NALP3 inflammasome through phagosomal destabilization. *Nat Immunol* 2008; **9**: 847–856.
30. Halle A, Hornung V, Petzold GC, Stewart CR, Monks BG, Reinheckel T *et al.* The NALP3 inflammasome is involved in the innate immune response to amyloid-beta. *Nat Immunol* 2008; **9**: 857–865.
31. Sin YM, Sedgwick AD, Chea EP, Willoughby DA. Mast cells in newly formed lining tissue during acute inflammation: a six day air pouch model in the mouse. *Ann Rheum Dis* 1986; **45**: 873–877.

Supplementary Information accompanies this paper on Cell Death and Disease website (http://www.nature.com/cddis)

Case Report

Dermatology

Dermatology 2013;227:26–30
DOI: 10.1159/000351323

Received: February 24, 2013
Accepted: March 17, 2013
Published online: August 8, 2013

A New Infant Case of Nakajo-Nishimura Syndrome with a Genetic Mutation in the Immunoproteasome Subunit: An Overlapping Entity with JMP and CANDLE Syndrome Related to *PSMB8* Mutations

Kayo Kunimoto[a, b] Ayako Kimura[a, b] Koji Uede[b] Masumi Okuda[c, d] Noriyuki Aoyagi[c] Fukumi Furukawa[a] Nobuo Kanazawa[a]

[a]Department of Dermatology, Wakayama Medical University, and Departments of [b]Dermatology and [c]Pediatrics, Wakayama Rosai Hospital, Wakayama, and [d]Department of Pediatrics, Sasayama Medical Center, Hyogo College of Medicine, Sasayama, Japan

Key Words
Nakajo-Nishimura syndrome · *PSMB8* mutation · Immunoproteasome · Partial lipodystrophy

Abstract
Nakajo-Nishimura syndrome (NNS) is a very rare hereditary autoinflammatory disorder that generally has its onset in infancy with pernio-like rashes and gradually develops into partial lipodystrophy. A distinct homozygous *PSMB8* mutation encoding an immunoproteasome subunit has recently been identified as its genetic cause. Here, we report a new case of a patient with NNS who developed exudative erythemas on his face and extremities at 2 months of age, along with high fever, elevated serum hepatic aminotransferase levels and hepatosplenomegaly. Massive infiltration of inflammatory cells was observed histologically in the dermis and subcutis without apparent leukocytoclastic vasculitis. These symptoms improved with oral corticosteroids but recurred periodically, and a thin angular face with long clubbed fingers gradually developed. Identification of the *PSMB8* mutation finalized the diagnosis of NNS at 5 years of age. Understanding a variety of clinicopathological features at the developmental stages is necessary to make an early diagnosis of NNS.

Introduction

Nakajo-Nishimura syndrome (NNS; OMIM #256040, ORPHA2615) is an autosomal, recessively inherited disorder which has been reported uniquely in Japan [1]. Patients with this disease show pernio-like skin rashes since infancy, and they gradually develop partial lipodystrophy mainly in the face and upper extremities, as well as characteristic long clubbed fingers with contracture of the interphalangeal joints accompanied by remittent fever and nodular erythema-like skin eruptions. Although a diagnosis of NNS is not difficult when the characteristic features are fully developed, it can be difficult soon after disease onset in infancy. Currently, more than 20 cases of NNS have been reported, but none of the patients were younger than 5 years when reported, except for the 8-month-old sister of an affected 10-year-old patient [2–6]. Recently, a homozygous missense mutation of the *PSMB8* gene, encoding the β5i subunit of immunoproteasome, has been identified to be responsible for NNS, and thus genetic analysis is expected to be the most reliable method for diagnosis [7, 8].

Here, we describe the detailed clinical observations of a new NNS case whose correct diagnosis was finally made at 5 years of age by genetic analysis. He was born more than 20 years after the birth of the last patient with NNS, and currently is the only living infant case in Japan.

Case Report

A 5-year-old Japanese boy, without parental consanguinity or any remarkable family history, presented with occasional periorbital pernio-like erythemas. He was delivered by cesarean section and received phototherapy for severe newborn jaundice, but no other remarkable abnormalities were observed around the time of his birth. Disease onset was at the age of 2 months, in the summertime, when exudative erythe-

KARGER

E-Mail karger@karger.com
www.karger.com/drm

1018–8665/13/2271–0026$38.00/0

Dr. Nobuo Kanazawa
Department of Dermatology, Wakayama Medical University
811-1 Kimiidera
Wakayama 641-0012 (Japan)
E-Mail nkanazaw@wakayama-med.ac.jp

mas appeared on his fingers and toes, accompanied by a high fever reaching 40°C. As the symptoms worsened despite the administration of oral antibiotics, he was referred to the Departments of Dermatology and Pediatrics of Wakayama Rosai Hospital at the age of 3 months. On examination, multiple swollen erythemas with central necrosis and ulcerations with diameters of several centimeters were observed not only on his fingers, toes, palms and soles, but also on his face and trunk (fig. 1). Laboratory investigations showed a high white blood cell count (13,400/mm^3) with lymphocytosis (neutrophils 18%, monocytes 7%, eosinophils 3%, lymphocytes 74%), slight anemia (hemoglobin 11.3 g/dl), a normal platelet count (326,000/mm^3), elevated levels of serum aspartate aminotransferase (141 IU/l; normal: 22–73 IU/l), alanine aminotransferase (215 IU/l; normal: 13–63 IU/l) and lactate dehydrogenase (424 IU/l; normal: 156–362 IU/l). In contrast, his serum alkaline phosphatase, γ-glutamyl transferase, creatinine, blood urea nitrogen, uric acid, creatine kinase and C-reactive protein levels were within normal ranges. Although neonatal lupus erythematosus was suspected, his serum antinuclear antibody, anti-Sm, anti-SS-A, anti-SS-B, anticardiolipin antibodies and cryoglobulin were all negative. Notably, his first infection with cytomegalovirus (CMV) was obvious, because both IgM and IgG antibodies were positive against CMV. Hepatosplenomegaly was observed by computed tomography (CT). A histopathologic examination of an erythematous lesion in his left palm at the age of 4 months revealed a massive infiltration of inflammatory cells from just below the epidermis to the subcutaneous adipose and deep striated muscle tissues (fig. 2a). In the dermis, the inflammatory cell infiltration was mainly observed around the vessels and adnexa, without any apparent leukocytoclastic vasculitis by neutrophilic infiltration (fig. 2b). Immunohistochemistry showed that the infiltrating cells were partly immunopositive for CD45RO and CD68, but immunonegative for CD1a, CD20, CD56 and S-100. Some of the mononuclear cells showed nuclear atypia but were considered to be reactive histiocytes without mitosis (fig. 2c). Although CMV antigen was immunohistochemically detected, neither apparent hemorrhage suggestive of acute hemorrhagic edema nor hemophagocytosis suggestive of cytophagic histiocytic panniculitis were found in the lesional skin. Bone

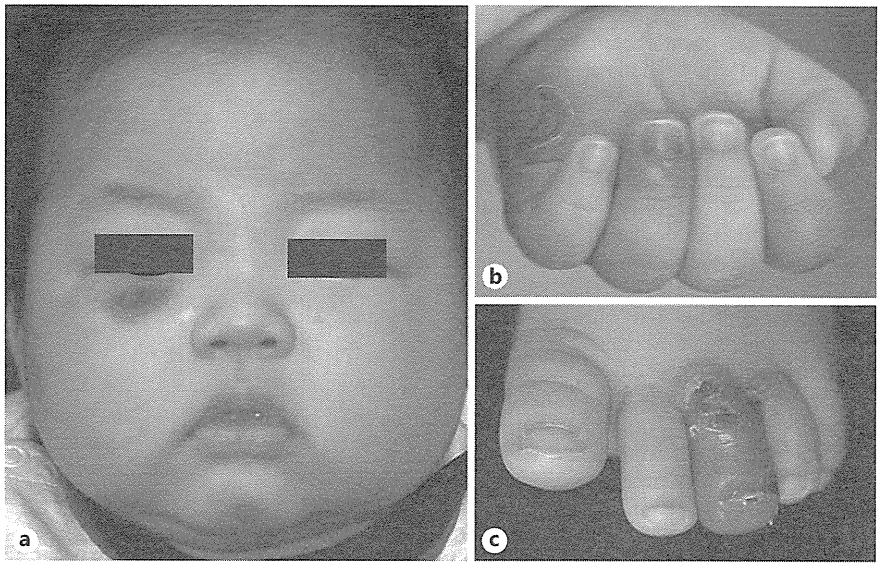

Fig. 1. Clinical photographs of the patient at 3 months of age. Multiple swollen erythemas with central necrosis or ulcerations on his face (**a**), hand (**b**) and foot (**c**) were observed.

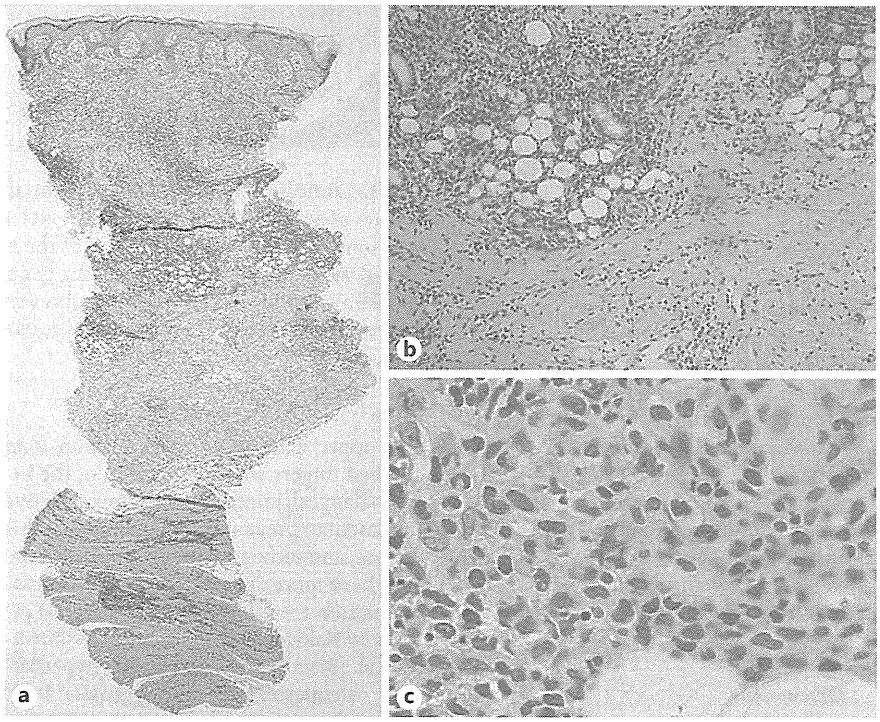

Fig. 2. Histopathological findings of erythematous lesions. The samples were obtained when the patient was 4 months (**a**, **b**) and 1 year (**c**) old. HE. Original magnifications: **a** ×20, **b** ×100, **c** ×400.

marrow aspiration revealed no hematologic abnormalities or malignancies. His thigh was examined with MRI to rule out dermatomyositis, but no remarkable changes were observed. Based on the observations that neither infectious nor malignant disorders were suspected, oral betamethasone (2 mg/day) was administered without a proper diagnosis at the age of 1 year. As expected, his skin eruptions and fever immediately disappeared, and the laboratory data became normal. However, these symptoms repeatedly recurred after tapering the medication, and oral betamethasone was administered intermittently at each flare-up. An analysis of his serum cytokine levels at 4 years of age revealed slightly high interleukin (IL)-6 (5.6 pg/ml; normal: <4.0 pg/ml), but his tumor necrosis factor-α, interferon-γ and IL-1β levels were normal.

Around the age of 5 years, his face gradually became angular and his fingers showed a mild deformity with swollen interphalangeal joints, which formed the characteristic appearance of long clubbed fingers (fig. 3a–c). On the suspicion of NNS, serial cranial CT scans were taken for the first time, and calcification of the basal ganglia, pons and white matter of the frontal lobe became apparent (fig. 3d). Furthermore, a genomic analysis of the patient and his parents was performed after informed consent was obtained according to the protocol approved by the ethics committee of Wakayama Medical University, and a c.602G>T mutation of the *PSMB8* gene causing the amino acid substitution of Gly201Val was homozygously detected in the patient, and heterozygously in his parents (fig. 3e). Since this mutation has been identified uniquely in NNS cases, his disease was finally confirmed as NNS. At the age of 6 years, methotrexate was further administered for the intractable skin rashes on his face. Notably, a severe worsening of laboratory findings was never experienced after the administration of oral corticosteroids, and methotrexate was effective against his skin lesions.

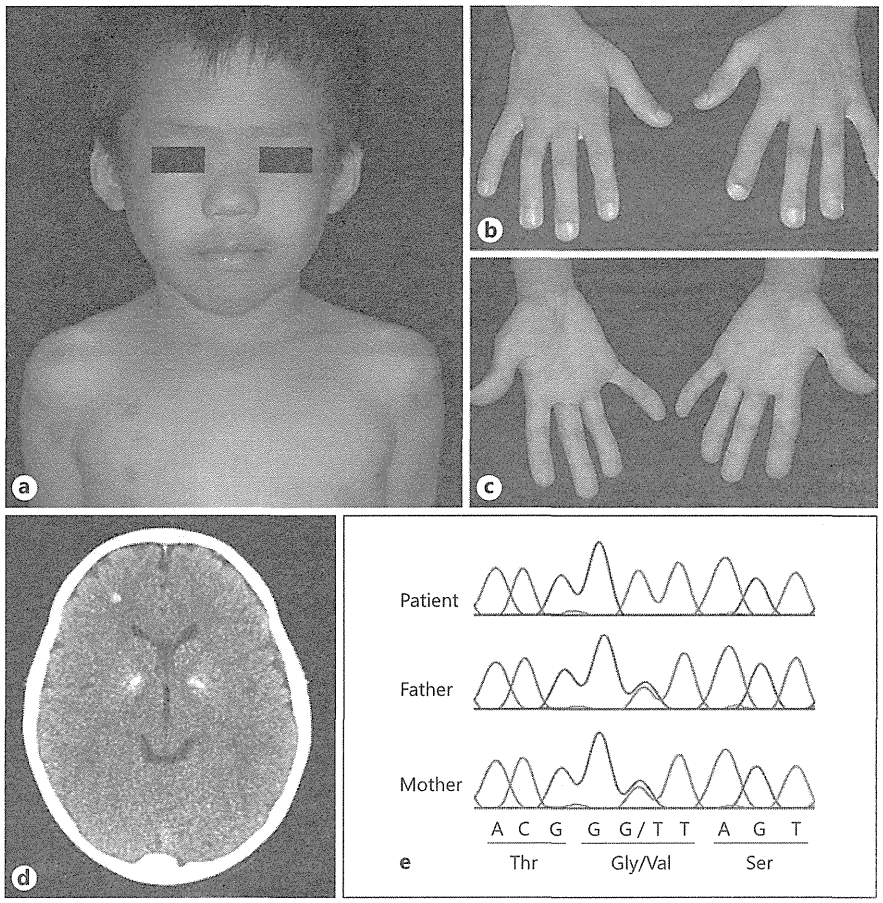

Fig. 3. Clinical photographs (**a–c**), cranial CT (**d**) and genomic analysis of the patient at 5 years of age (**e**). A thin angular face (**a**), long clubbed fingers with swollen interphalangeal joints (**b**, **c**) and calcification of the basal ganglia on cranial CT scans (**d**) were observed. **e** Electrophoretograms of the genomic sequence of the patient and his parents. A c.602G>T mutation causing an amino acid substitution of Gly201Val was found homozygously in this patient and heterozygously in both parents.

Discussion

NNS is a hereditary disorder that has its onset in infancy with pernio-like skin rashes, and is accompanied by remittent fever and nodular erythema-like skin eruptions [1]. Patients with NNS gradually develop a partial lipodystrophy, mainly in the face and upper extremities, and develop long clubbed fingers with contracture of the interphalangeal joints. There is no effective treatment to prevent the progression of this disease, and some patients die young. There have been more than 20 reports of NNS cases uniquely from Japan since the earliest reports by Nakajo [2] in 1939 and by Nishimura et al. [3] in 1950 as 'secondary hypertrophic osteoperiostosis with pernio' [4–6]. Due to the phenotypic similarities, NNS is considered to be a new member of the family of hereditary autoinflammatory disorders.

According to a review of all 28 reported cases with NNS, 8 features were selected for a tentative checklist of diagnostic criteria, and the detection of at least 5 features was defined to be sufficient for a clinical diagnosis of NNS (table 1) [1]. As 7 out of the 8 features were observed in our case, except for the autosomal recessive inheritance, our case can be clinically diagnosed as NNS. However, before the partial lipomuscular atrophy with characteristic long clubbed fingers became noticeable at 5 years of age, he had shown only 4 features (pernio-like rashes, nodular erythema-like eruptions, periodic fever and hepatosplenomegaly). Therefore, head CT scanning in search for basal ganglion calcification is a critical step for an early diagnosis of NNS. Furthermore, the establishment of a serum marker or simple examination

would be expected for an objective estimation of partial lipodystrophy. As a result of a national survey on NNS in Japan which had recently been performed using these criteria, 11 cases have been confirmed to be still alive, including our case. Notably, our patient is the only infant case who was born more than 20 years after the birth of the last NNS case [1].

Recently, Arima et al. [7] and Kitamura et al. [8] independently reported the identification of a homozygous c.602G>T mutation in the *PSMB8* gene encoding the immunoproteasome β5i subunit in NNS patients by homozygosity mapping. This mutation has been homozygously detected uniquely in all NNS cases investigated, including the present case. The resulting Gly201Val substitution causes the defective assembly of the immunoproteasome complex and severe defects in proteasome activities overall. Accordingly, detection of the *PSMB8* gene mutation is expected to confirm the diagnosis of NNS.

Although NNS has been assumed to be found exclusively in Japan, several cases of new syndromes presenting with similar clinical features and other *PSMB8* mutations have successively been reported from foreign countries [9–13]. Three cases were reported as JMP (joint contractures, muscular atrophy, microcytic anemia and panniculitis-induced lipodystrophy) syndrome harboring a homozygous mutation of c.224C>T in the *PSMB8* gene with a T75M amino acid transition, whereas another 8 cases were designated as CANDLE (chronic atypical neutrophilic dermatosis with lipodystrophy and elevated temperature) syndrome harboring a homozygous or heterozygous c.224C>T mutation, or a homozygous nonsense mutation of c.405C>A with a premature termination (C135X). In contrast to patients with JMP syndrome, who showed seizures without pernio-like rashes or recurrent fever, patients with CANDLE syndrome showed all 8 features of the list of criteria for a clinical diagnosis of NNS, and they looked quite similar to patients with this disease [9, 11–13]. Histologically, the massive infiltration of activated neutrophils into the dermis was reported to be highly characteristic of CANDLE syndrome, whereas such a feature was not observed in our case [11–13]. Actually, a palpable erythema on the chest showing inflammatory cell infiltration in the upper dermis without leukocytoclastic vasculitis was further analyzed immunohistochemically at 6 years of age, and the infiltrating cells were positive for myeloperoxidase but immunonegative for CD15, a marker of mature neutrophils (data not shown). Collectively, it appears that these related disorders with *PSMB8* mutations may be categorized as a novel class of hereditary autoinflammatory diseases, namely proteasome disability syndromes, and they might be subdivided by clinical, histologic and genetic features. To determine the precise genotype-phenotype correlations, the analysis of a greater number of cases would be required.

It took almost 5 years to make a proper diagnosis in our case. The clinical diagnostic criteria and genetic analysis were both useful, but they would not be routinely performed unless the disease was suspected. In order to determine the diagnosis of this disease and to start therapy before progression to lipomuscular atrophy or joint contracture, it is important to understand the variety of clinicopathological features.

Table 1. Tentative criteria for the clinical diagnosis of NNS

1	Autosomal recessive inheritance (parental consanguinity and/or familial occurrence)
2	Pernio-like purplish rashes on hands and feet (appearing in winter since infancy)
3	Haunting nodular erythema with infiltration and induration (sometimes circumscribed)
4	Repetitive spiking fever (periodic, not necessarily)
5	Long clubbed fingers and toes with joint contractures
6	Progressive partial lipomuscular atrophy and emaciation (marked in upper part of body)
7	Hepatosplenomegaly
8	Basal ganglion calcification

A clinical diagnosis of NNS can be made if at least 5 of the 8 features above are positive and other diseases are excluded.

Acknowledgments

This study was supported by grants from the Ministry of Health, Labor and Welfare of Japan, and the Japan Society for the Promotion of Science for K.K. and N.K.

Disclosure Statement

The authors have no conflicts of interest to declare.

References

1 Kanazawa N: Nakajo-Nishimura syndrome: an autoinflammatory disorder showing pernio-like rashes and progressive partial lipodystrophy. Allergol Int 2012;61:197–206.

2 Nakajo A: Secondary hypertrophic osteoperiostosis with pernio (in Japanese). Jap J Dermatol Urol 1939;45:77–86.

3 Nishimura N, Deki T, Kato S: Secondary hypertrophic osteoperiostosis with pernio-like skin lesions observed in two families (in Japanese). Jap J Dermatol Venereol 1950;60:136–141.

4 Kitano Y, Matsunaga E, Morimoto T, Okada N, Sano S: A syndrome with nodular erythema, elongated and thickened fingers, and emaciation. Arch Dermatol 1985;121:1053–1056.

5 Tanaka M, Miyatani N, Yamada S, Miyashita K, Toyoshima I, Sakuma K, Tanaka K, Yuasa T, Miyatake T, Tsubaki T: Hereditary lipomuscular atrophy with joint contracture, skin eruptions and hyper-γ-globulinemia: a new syndrome. Intern Med 1993;32:42–45.

▶6 Kasagi S, Kawano S, Nakazawa T, Sugino H, Koshiba M, Ichinose K, Ida H, Eguchi K, Kumagai S: A case of periodic-fever-syndrome-like disorder with lipodystrophy, myositis, and autoimmune abnormalities. Mod Rheumatol 2008;18:203–207.
▶7 Arima K, Kinoshita A, Mishima H, Kanazawa N, Kaneko T, Mizushima T, Ichinose K, Nakamura H, Tsujino A, Kawakami A, Matsunaka M, Kasagi S, Kawano S, Kumagai S, Ohmura K, Mimori T, Hirano M, Ueno S, Tanaka K, Tanaka M, Toyoshima I, Sugino H, Yamakawa A, Tanaka K, Niikawa N, Furukawa F, Murata S, Eguchi K, Ida H, Yoshiura K: Proteasome assembly defect due to a proteasome subunit beta type 8 *(PSMB8)* mutation causes the autoinflammatory disorder, Nakajo-Nishimura syndrome. Proc Natl Acad Sci USA 2011;108:14914–14919.
▶8 Kitamura A, Maekawa Y, Uehara H, Izumi K, Kawachi I, Nishizawa M, Toyoshima Y, Takahashi H, Standley DM, Tanaka K, Hamazaki J, Murata S, Obara K, Toyoshima I, Yasutomo K: A mutation in the immunoproteasome subunit *PSMB8* causes autoinflammation and lipodystrophy in humans. J Clin Invest 2011; 121:4150–4160.
▶9 Garg A, Hernandez MD, Sousa AB, Subramanyam L, Martínez de Villarreal L, dos Santos HG, Barboza O: An autosomal recessive syndrome of joint contracture, muscular atrophy, microcytic anemia, and panniculitis-associated lipodystrophy. J Clin Endocrinol Metab 2010;95:E58–E63.
▶10 Agarwal AK, Xing C, DeMartino GN, Mizrachi D, Hernandez MD, Sousa AB, Martínez de Villarreal L, dos Santos HG, Garg A: *PSMB8* encoding the β5i proteasome subunit is mutated in joint contractures, muscle atrophy, microcytic anemia, and panniculitis-induced lipodystrophy syndrome. Am J Hum Genet 2010;87:866–872.
▶11 Torrelo A, Patel S, Colmenero I, Gurbindo D, Lendínez F, Hernández A, López-Robledillo JC, Dadban A, Requena L, Paller AS: Chronic atypical neutrophilic dermatosis with lipodystrophy and elevated temperature (CANDLE) syndrome. J Am Acad Dermatol 2010; 62:489–495.
▶12 Ramot Y, Czarnowicki T, Maly A, Navon-Elkan P, Zlotogorski A: Chronic atypical neutrophilic dermatosis with lipodystrophy and elevated temperature syndrome: a case report. Pediatr Dermatol 2011;28:538–541.
▶13 Liu Y, Ramot Y, Torrelo A, Paller AS, Si N, Babay S, Kim PW, Sheikh A, Lee CC, Chen Y, Vera A, Zhang X, Goldbach-Mansky R, Zlotogorski A: Mutations in proteasome subunit β type 8 cause chronic atypical neutrophilic dermatosis with lipodystrophy and elevated temperature with evidence of genetic and phenotypic heterogeneity. Arthritis Rheum 2012;64:895–907.

Mol Biol Rep (2014) 41:545–553
DOI 10.1007/s11033-013-2890-y

Defect of suppression of inflammasome-independent interleukin-8 secretion from SW982 synovial sarcoma cells by familial Mediterranean fever-derived pyrin mutations

Rino Sugiyama · Kazunaga Agematsu · Kiyoshi Migita · Jun Nakayama · Sho Mokuda · Fumiya Ogura · Kaho Haraikawa · Chikara Okumura · Satomi Suehiro · Shinnosuke Morikawa · Yuki Ito · Junya Masumoto

Received: 23 October 2012 / Accepted: 30 November 2013 / Published online: 7 December 2013

Abstract Familial Mediterranean fever (FMF) is a recessive inherited autoinflammatory syndrome. Patients with FMF have symptoms such as recurrent fever and abdominal pain, sometimes accompanied by arthralgia. Biopsy specimens have revealed substantial neutrophil infiltration into synovia. FMF patients have a mutation in the Mediterranean fever gene, encoding pyrin, which is known to regulate the inflammasome, a platform for processing interleukin (IL)-1β. FMF patients heterozygous for E148Q mutation, heterozygous for M694I mutation, or combined heterozygous for E148Q and M694I mutations, which were found to be major mutations in an FMF study group in Japan, suffer from arthritis, the severity of which is likely to be lower than in FMF patients with M694V mutations. Expression plasmids of wild-type (WT) pyrin and mutated pyrin, such as E148Q, M694I, M694V, and E148Q+M694I, were constructed, and SW982 synovial sarcoma cells were transfected with these expression plasmids. IL-8 and IL-6 were spontaneously secreted from the culture supernatant of SW982 cells without any stimulation, whereas IL-1β and TNF-α could not be detected even when stimulated with lipopolysaccharide. Notably, two inflammasome components, ASC and caspase-1, could not be detected in SW982 cells by Western blotting. IL-8 but not IL-6 secretion from SW982 cells was largely suppressed by WT pyrin, but less suppressed by mutated pyrin, which appeared to become weaker in the order of E148Q, M694I, E148Q+M694I, and M694V mutations. As for IL-8 and IL-6, similar results were obtained using stable THP-1 cells expressing the WT pyrin or mutated pyrins, such as M694V or E148Q, when stimulated by LPS. In addition, IL-8 secretion from mononuclear cells of FMF patients was significantly higher than that of healthy volunteers when incubated on a culture plate. Thus, our results suggest that IL-8 secretion from SW982 synovial sarcoma cells suppressed by pyrin independently of inflammasome is affected by pyrin mutations, which may reflect the activity in FMF arthritis.

Keywords Pyrin · Familial Mediterranean fever · Interleukin-8 · Synovial sarcoma · SW982

R. Sugiyama · J. Nakayama · J. Masumoto
Department of Molecular Pathology, Shinshu University Graduate School of Medicine, Matsumoto, Nagano 390-8621, Japan

K. Agematsu
Department of Infectious Immunology, Shinshu University Graduate School of Medicine, Matsumoto, Nagano 390-8621, Japan

K. Migita
Clinical Research Center, Nagasaki Medical Center, Ōmura, Nagasaki 856-8562, Japan

S. Mokuda · F. Ogura · K. Haraikawa · C. Okumura · S. Suehiro · S. Morikawa · Y. Ito · J. Masumoto (✉)
Department of Pathology, Ehime University Proteo-Science Center and Graduate School of Medicine, Shitsukawa 454, Toon, Ehime 791-0295, Japan
e-mail: masumoto@m.ehime-u.ac.jp

Introduction

Familial Mediterranean fever (FMF) (OMIM#249100) is an autosomal recessive inherited autoinflammatory syndrome [1]. Patients with FMF have symptoms such as recurrent fever and abdominal pain, sometimes accompanied by arthralgia [1]. Patient biopsies have revealed that the cause is arthritis, involving neutrophils infiltrating into synovium [2]. Patients have a mutation in the Mediterranean fever (*MEFV*)

gene, encoding pyrin, which is known to regulate the inflammasome, a platform for processing interleukin (IL)-1β [3–5].

In Middle Eastern countries, FMF patients homozygous for M694V suffer a severe form of the disease, with clinical manifestations including arthritis, while the condition of FMF patients homozygous for M694I, one of the major mutations in Japan, is not so severe [6–8]. In Japan, there were no FMF patients with M694V mutation found by the Japan study group of FMF patients [9]. FMF patients heterozygous for E148Q, heterozygous for M694I, or combined-heterozygous for E148Q and M694I suffer from arthritis, and the severity of E148Q was reported to be lower than in FMF patients with M694V [10]. Interestingly, there was reported to be a corelationship between the concomitant expression of *MEFV* and C5a/IL-8-inhibitor activity in primary cultures of human fibroblasts [11].

Activation of inflammasome is reported to lead to IL-8 production from some cells, as well as that of IL-1β [12]. IL-8 is a chemotactic factor for neutrophils and enhances the trans-endothelial migration of neutrophils by inducing rapid shedding of L-selectin [13, 14]. Focal IL-8 secretion may reflect disease activity [15]. These facts prompted us to evaluate IL-8 secretion from synovial cells.

In this study, we evaluated the secretion of cytokines such as IL-1β, IL-6, IL-8, and TNF-α secretion from synovial sarcoma SW982 cells and monocytic leukemia THP-1 cells transfected with expression plasmids encoding wild-type (WT) pyrin and E148Q, M694V, M694I, and E148Q+M694I mutated pyrin in order to obtain new insight into FMF arthritis. Then, we also confirmed the results were reflected clinically in FMF patients.

Materials and methods

Preparation of expression plasmids

Expression plasmids encoding M694V, M694I, E148Q, E148Q+M694I, or WT pyrin were constructed as follows. The entire open reading frame of pyrin was inserted into the *EcoRI* and *BglII* sites of pFLAG-CMV-4 (Vector) (Sigma-Aldrich, St. Louis, MO, USA) to produce pFLAG-CMV-4-pyrin-WT from pcDNA3-HA-pyrin-WT as a template by polymerase chain reaction (PCR) using primer sets as follows: forward primer Pyrin-EcoRI-F 5-GCGAATTCAGCTAAGACCCCTAGTGACCAT-3 and reverse primer Pyrin-BglII-R 5-GTCAGATCTTCAGTCAGGCCCCTGACCACC-3 [16, 17]. PCR-based site-specific mutagenesis for pFLAG-CMV-4-pyrin-E148Q was generated by two-step PCR using primer sets as follows: forward primer Pyrin-EcoRI-F 5-GCGAATTCAGCTAAGACCCCTAGTGACCAT-3 and reverse primer Pyrin-E148Q-R 5-GGTGCAGCCAGCCCCAGGCCGGGAGGGGGC-3, and forward primer Pyrin-E148Q-F 5-GCCCCCTCCCGGCCTGGGGCTGGCTGCACC-3 and reverse primer Pyrin-BglII-R 5-GTCAGATCTTCAGTCAGGCCCCTGACCACC-3 for the first over-lapping DNA fragment set from pcDNA3-HA-pyrin-WT plasmid as a template [16, 17]. Full-length E148Q mutated-pyrin DNA fragment was amplified by second PCR using a primer set as follows: forward primer Pyrin-EcoRI-F 5-GCGAATTCAGCTAAGACCCCTAGTGACCAT-3 and reverse primer Pyrin-BglII-R 5-GTCAGATCTTCAGTCAGGCCCCTGACCACC-3 from the first over-lapping DNA fragment set as templates, and then inserted into the *EcoRI* and *BglII* sites of pFLAG-CMV-4. pFLAG-CMV-4-pyrin-M694V and pFLAG-CMV-4-pyrin-M694I were generated by the same method. pFLAG-CMV-4-pyrin-E148Q+M694I was also generated by the same method from pFLAG-CMV-4-pyrin-E148Q as a template. Primers and oligonucleotide sequences are listed in Table 1. Mutations were confirmed by sequencing (Fig. 1a).

Transfection of expression plasmids, their expression and generation of THP-1 stable cells

5×10^6 human embryonic kidney (HEK) 293T cells were transfected with 3 μg of pFLAG-CMV-4 (Vector), pFLAG-CMV-4-pyrin-WT, pFLAG-CMV-4-pyrin-E148Q, pFLAG-CMV-4-pyrin-M694I, pFLAG-CMV-4-pyrin-M694V, or pFLAG-CMV-4-pyrin-E148Q+M694I using the calcium phosphate method as described previously [18]. 36 h after transfection, each protein's expression was detected by Western blotting. 5×10^6 synovial sarcoma SW982 cells were transfected with pFLAG-CMV-4 (Vector), pFLAG-CMV-4-pyrin-WT, pFLAG-CMV-4-pyrin-E148Q, pFLAG-CMV-4-pyrin-M694I, pFLAG-CMV-4-pyrin-M694V, or pFLAG-CMV-4-pyrin-E148Q+M694I using Lipofectamine™ 2000 (Invitrogen, Grand Island, NY, USA) as per the manufacturer's instructions. 1×10^7

Table 1 Primers and oligonucleotide sequences for site-specific mutagenesis of pyrin plasmids

Name	Oligo-nucleotide-sequence
Pyrin-EcoRI-F	5′ GCGAATTCAGCTAAGACCCCTAGTGACCAT 3′
Pyrin-BglII-R	5′ GTCAGATCTTCAGTCAGGCCCCTGACCACC 3′
Pyrin-E148Q-F	5′GGTGCAGCCAGCCCCAGGCCGGGAGGGGGC 3′
Pyrin-E148Q-R	5′GCCCCCTCCCGGCCTGGGGCTGGCTGCACC 3′
Pyrin-M694I-F	5′GGTGGTGATAATGATCAAGGAAAATGAGTA 3′
Pyrin-M694I-R	5′TACTCATTTTCCTTGATCATTATCACCACC 3′
Pyrin-M694V-F	5′GGTGGTGATAATGGTGAAGGAAAATGAGTA 3′
Pyrin-M694V-R	5′TACTCATTTTCCTTCACCATTATCACCACC 3′

Underlines indicate mutation codons for specific amino acids

Double underlines indicate restriction enzyme sites

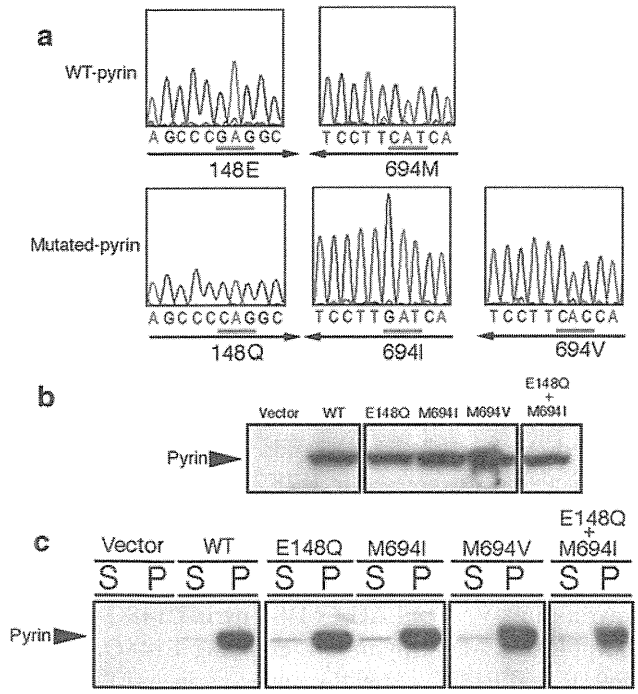

Fig. 1 Chart of sequencing of mutated pyrin plasmids, expression, and fractionation in human embryonic kidney 293T cells. **a** The mutated-pyrin expression plasmids pFLAG-CMV-4-pyrin E148Q, pFLAG-CMV-4-pyrin M694I, and pFLAG-CMV-4-pyrin M694V were sequenced to confirm (from GAG to CAG corresponding to E148Q; from complementary CAT to GAT corresponding to M694I; from complementary CAT to CAC corresponding to M694I) mutations in the appropriate site. **b** 5×10^6 human embryonic kidney 293T cells were transfected with 3 μg of pFLAG-CMV-4 (Vector), pFLAG-CMV-4-pyrin-WT, pFLAG-CMV-4-pyrin E148Q, pFLAG-CMV-4-pyrin-M694I, pFLAG-CMV-4-pyrin-M694V, and pFLAG-CMV-4-pyrin-E148Q+M694I. 36 h after transfection, 30 μg of each whole cell lysate was subjected to Western blotting. **c** 5×10^6 human embryonic kidney 293T cells were transfected with 3 μg of pFLAG-CMV-4 (Vector), pFLAG-CMV-4-pyrin-WT, pFLAG-CMV-4-pyrin E148Q, pFLAG-CMV-4-pyrin-M694I, pFLAG-CMV-4-pyrin-M694V, and pFLAG-CMV-4-pyrin-E148Q+M694I. 36 h after transfection, the cells were lysed in 1 % (v/v) NP-40 buffer and fractionated into soluble (*S* supernatant) and insoluble (*P* pellet) fraction. 30 μg of each fractionated protein was subjected to Western blotting

monocytic leukemia THP-1 cells were transfected with 5 μg of pFLAG-CMV-4 (Vector), pFLAG-CMV-4-pyrin-WT, pFLAG-CMV-4-pyrin-E148Q, or pFLAG-CMV-4-pyrin-M694V, using the Amaxa® Nucleofector as per the manufacturer's instructions. After incubation with 500 μg/ml G418 (Sigma) in RPMI 1640 medium including 10 % fetal bovine serum (FBS) (Defined, endotoxin ≦10 EU/ml; Thermo Scientific HyClone, South Logan, UT, USA) for 4 weeks at 37 °C in a humidified atmosphere with 5 % CO_2, THP-1 stable cells expressing WT or mutated pyrin protein were generated.

Fractionation of cell lysates

5×10^6 HEK293T cells were transfected with 3 μg of pFLAG-CMV-4 (Vector), pFLAG-CMV-4-pyrin-WT, pFLAG-CMV-4-pyrin-E148Q, pFLAG-CMV-4-pyrin-M694I, pFLAG-CMV-4-pyrin-M694V, and pFLAG-CMV-4-pyrin-E148Q+M694I. 36 h after transfection, the cells were lysed in 1.0 % (v/v) NP-40 buffer (1 % Nonidet P-40, 142.5 mM KCl, 5 mM MgCl–$6H_2O$, 10 mM HEPES [pH 7.6], 0.2 mM PMSF, 1 mM EDTA) with proteinase inhibitor cocktail Complete™ (Roche Molecular Biochemicals, Mannheim, Germany). The lysate was fully dislodged from the plate surface with a rubber policeman. The lysate from one dish was incubated in a 1.5-ml tube on ice, clarified by centrifugation at 12,000 rpm for 20 min, and separated into soluble (S: supernatant) and insoluble (P: pellet) fractions. Both fractions of the whole cell lysate were subjected to Western blotting using anti-pyrin polyclonal antibody (AL196; ALEXIS Biochemical, Lausen, Switzerland) (Fig. 1c).

Measurement of cytokine secretion from synovial sarcoma SW982 cells and monocytic leukemia THP-1 cells

Human synovial sarcoma SW982 cells and monocytic leukemia THP-1 cells were purchased from American Type Culture Collection, and pre-cultured in 12-well flat-bottomed plates (BD Biosciences, San Jose, CA, USA) to a final cell density of 1×10^6/ml in a volume of 1 ml of Dulbecco's modified Eagle's medium (DMEM; Invitrogen, Grand Island, NY, USA), including 10 % fetal FBS, for 24 h at 37 °C in a humidified atmosphere with 5 % CO_2. The cells in each well were transfected with 1.67 μg of expression plasmids in the presence of 0.67 μg of pEF1-BOS-β-gal. 8 h after transfection, culture medium was replaced by 1 ml of DMEM alone, or DMEM containing 1.0 ng/ml or 1.0 μg/ml of lipopolysaccharide (LPS) (from *Escherichia coli* O55:B5, cell culture tested, purified by phenol extraction; Sigma-Aldrich, St. Louis, MO, USA). 8 h after medium replacement, the concentrations of IL-1β, IL-6, IL-8, and TNF-α in the culture supernatant were measured by enzyme-linked immunosorbent assay (ELISA) with specific antibodies (BD Biosciences, San Jose, CA, USA). Percentiles of IL-8-related-suppression ratio of mutated pyrin versus WT pyrin were normalized to the transfection efficiency by β-galactosidase activity from triplicate experiments. THP-1-derived stable cells expressing WT or mutated pyrin proteins were pre-cultured in 24-well flat-bottomed plates (BD Biosciences, San Jose, CA, USA) to a final cell density of 2×10^7/ml in a volume

of 300 μl of RPMI1640 Medium (Invitrogen, Grand Island, NY, USA), including 10 % FBS, for 24 h at 37 °C in a humidified atmosphere with 5 % CO_2. Then, culture medium was replaced with 300 μl of RPMI1640 containing 10 ng/ml LPS. 8 h after medium replacement, the concentrations of IL-1β, IL-6, IL-8, and TNF-α in the culture supernatant were measured by ELISA with specific antibodies (BD Biosciences, San Jose, CA, USA).

Western blotting analyses for p38, ERK, and NF-κB pathways

40 μg of SW982 cell lysates were subjected to SDS-PAGE followed by Western blotting analysis for p38, ERK, and NF-κB, pathways. Signals from the same blotting membrane were detected by Phospho-p38 MAPK (Thr180/Tyr182) (D3F9) XP rabbit monoclonal antibody (Cell Signaling catalog No. #4511) and the p38α MAPK rabbit polyclonal antibody (Cell Signaling catalog No. #9218) for p38 MAPK pathway, or Phospho-p44/42 MAPK (Erk1/2) (Thr202/Tyr204) (D13.14.4E) XP rabbit monoclonal antibody (Cell Signaling catalog No. #4370) and p44/42 MAPK (Erk1/2) (137F5) rabbit monoclonal antibody (Cell Signaling catalog No. #4695) for the ERK pathway, or phospho-NF-κB p65 (Ser536) rabbit polyclonal antibody (Cell Signaling catalog No. #3031) and NF-κB p65 (D14E12) XP rabbit monoclonal antibodies (Cell Signaling catalog No. #8242) for the NF-κB pathway.

Cytokine assays for peripheral blood mononuclear cells

Participation of FMF patients and almost age-matched healthy volunteers regarding the analyses of *MEFV* gene and their blood samples with their written informed consents was approved by the institutional review board at the Shinshu University. We obtained peripheral blood mononuclear cells from five FMF patients with definite diagnosis as FMF according to the 'Tel Hashomer' criteria presented a symptom with typical type of FMF, and exhibited a favorable response to colchicine. All of them had *MEFV* mutations; four patients were E148Q/M694I compound heterozygotes (a 30-years-old woman, an 8-years-old boy, a 25-years-old woman and a 22-years-old woman) and one patient was an E148Q/E148Q homozygote (a 7-years-old girl). 5×10^5/ml of peripheral blood mononuclear cells were incubated in 96-well flat plates (Nunc) with RPMI1640 with 10 % heat-inactivated FBS for 6 h. The supernatants were collected and analyzed for cytokine concentration with the Cytometric Bead Array Flex set (BD Biosciences) according to the manufacturer's instructions. For intracellular cytokine staining, 5×10^5/ml of mononuclear cells including BD GolgiPlug protein transport inhibitor (BD Biosciences) were incubated under the same conditions as described above. After 6 h of incubation, adherent cells were collected by pipetting. The cells were fixed using a BD Cytofix/Cytoperm solution for 20 min at 4 °C, then the fixed cells were permeabilized by washing two times in 1 × BD Perm/Wash buffer. Intracellular IL-8 was stained with FITC-conjugated anti-IL-8 monoclona antibody (BioLegend) and APC-conjugated anti-IL-1β monoclona antibody (BioLegend) at 4 °C for 30 min. After washing with 1 × BD Perm/Wash buffer, resuspension in 1 × PBS was carried out, followed by flow cytometric analysis with a FACSCalibur flow cytometer.

Results

Mutated-pyrin expression plasmids were successfully constructed and expressed in HEK293T cells

Site-specific mutagenesis of plasmids, pFLAG-CMV-4-pyrin-E148Q, pFLAG-CMV-4-pyrin-M694I, pFLAG-CMV-4-pyrin-M694V, pFLAG-CMV-4-pyrin-E148Q+M694I, and pFLAG-CMV-4-pyrin-WT encoding E148Q, M694I, M694V, and E148Q+M694I mutated-pyrin and WT pyrin, generated from pcDNA3-HA-pyrin-WT as a template, was successfully completed and confirmed by sequencing (Fig. 1a). WT pyrin and E148Q, M694I, M694V, and E148Q+M694I mutated pyrin were stably expressed in HEK293T cells transfected with pFLAG-CMV-4-pyrin-WT, pFLAG-CMV-4-pyrin-E148Q, pFLAG-CMV-4-pyrin-M694I, pFLAG-CMV-4-pyrin-M694V, and pFLAG-CMV-4-pyrin-E148Q+M694I, whereas there was an undetectable level of pyrin in HEK293T cells transfected with pFLAG-CMV-4 (Vector) (Fig. 1b).

Wild-type pyrin and E148Q, M694I, M694V, and E148Q+M694I pyrin are detergent-insoluble

HEK293T cells were transfected with the expression plasmids pFLAG-CMV-4-pyrin-WT, pFLAG-CMV-4-pyrin-E148Q, pFLAG-CMV-4-pyrin-M694I, pFLAG-CMV-4-pyrin-M694V, or pFLAG-CMV-4-pyrin-E148Q+M694I, encoding WT, E148Q, M694I, M694V, and E148Q+M694I pyrin, respectively. The cells were suspended in 1.0 % NP-40 buffer and separated into soluble (S: supernatant) and insoluble (P: pellet) fractions by centrifugation at 12,000 rpm for 20 min. Both fractions were subjected to Western blotting. WT pyrin and all mutated pyrins that we tested were fractionated in detergent-insoluble fractions (Fig. 1c; P).

Cytokine secretion from synovial sarcoma SW982 cells

IL-8 and IL-6 were spontaneously secreted from synovial sarcoma SW982 cells (Fig. 2a, b), whereas IL-1β or TNF-α

could not be detected in our ELISA system even when stimulated by LPS (data not shown).

IL-8 secretion from SW982 cells was suppressed by WT pyrin but suppressed much less by mutated pyrins

When SW982 cells were transfected with expression plasmids pFLAG-CMV-4 (Vector), pFLAG-CMV-4-pyrin-E148Q, pFLAG-CMV-4-pyrin-M694I, pFLAG-CMV-4-pyrin-M694V, pFLAG-CMV-4-pyrin-E148Q+M694I, and pFLAG-CMV-4-pyrin-WT, IL-8 but not IL-6 secretion from SW982 seemed to be suppressed (Fig. 2a, b). After standardation to the β-galactosidase activity, related % of IL-8 secretion versus WT pyrin suppression, IL-8 secretion was significantly suppressed by WT pyrin but suppressed much less by E148Q, M694I, M694V, and E148Q+M694I pyrin in that order (Fig. 2c). In terms of IL-6 secretion from SW982 cells, there was no significant difference among all the mutations (Fig. 2d).

Neither ASC nor caspase-1 was expressed in 982 synovial sarcoma cells

The expressions of inflammasome components ASC and caspase-1 were analyzed by Western blotting. Although both ASC and caspase-1 were expressed in THP-1 monocytic leukemia cells, they were not expressed in SW982 cells as well as HEK293T cells (Fig. 3).

IL-1β, IL-8, TNF-α but not IL-6 secretion from THP-1 cells was suppressed by stably expressed WT pyrin but suppressed much less by stably expressed mutated pyrin proteins

We generated stable THP-1 cells transfected with expression plasmids pFLAG-CMV-4 (Vector), pFLAG-CMV-4-pyrin-E148Q, pFLAG-CMV-4-pyrin-M694 V, and pFLAG-CMV-4-pyrin-WT, which express no pyrin (vector control), or stably express mutant pyrin proteins such as M694V, E148Q, or WT pyrin (Fig. 4a inset). These cells secreted IL-

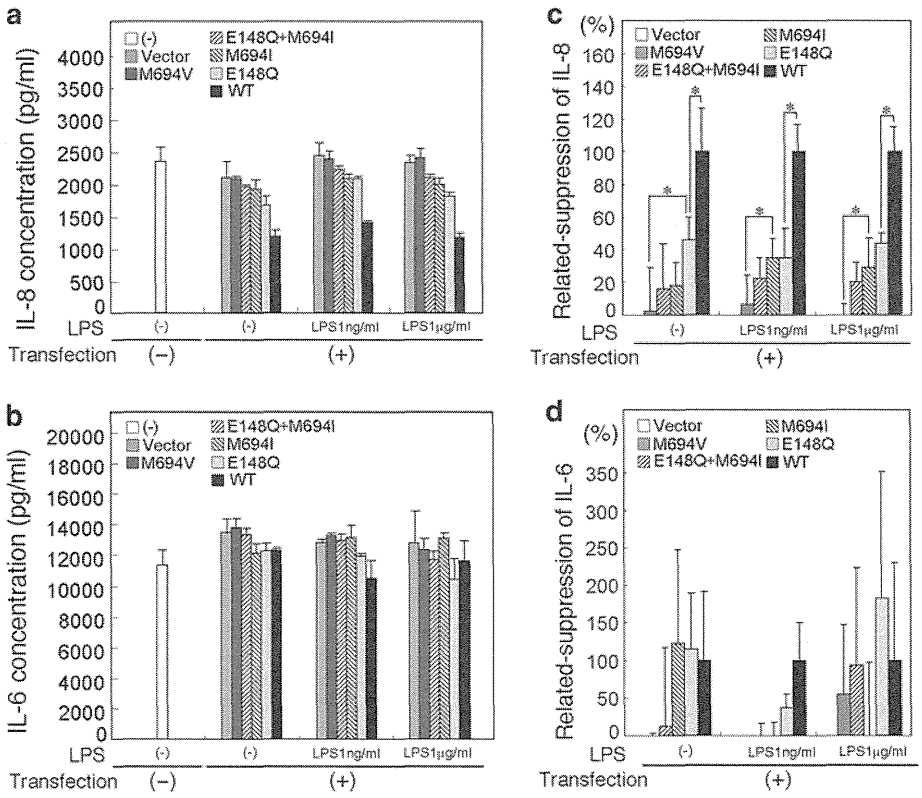

Fig. 2 Interleukin-8 and interleukin-6 secretion from SW982 synovial sarcoma cells transfected with expression plasmids. **a**, **b** 1×10^6 SW982 cells were transfected with 1.67 μg of pFLAG-CMV-4 (Vector), pFLAG-CMV-4-pyrin-M694V (M694V), pFLAG-CMV-4-pyrin-E148Q+M694I (E148Q+M694I), pFLAG-CMV-4-pyrin-M694I (M694I), pFLAG-CMV-4-pyrin-E148Q (E148Q), pFLAG-CMV-4-pyrin-WT (WT), or left untransfected (−) in the presence of 0.67 μg of pEF1-BOS-β-gal. 8 h after transfection, culture medium was replaced with 1 ml of DMEM alone [LPS(−)], or DMEM containing 1.0 ng/ml or 1.0 μg/ml LPS. 8 h after medium replacement, concentrations of interleukin-8 (IL-8) (**a**) and interleukin-6 (IL-6) (**b**) in the culture supernatant were measured by ELISA. Values are from triplicate cultures. **c**, **d** Percentiles are relative suppression of mutated pyrin versus WT pyrin. Percentiles of relative suppression of IL-8 (**c**) or IL-6 (**d**) secretion from SW982 cells transfected with mutated pyrin versus WT pyrin were normalized to the transfection efficiency by β-galactosidase activity from triplicate cultures. *A p value <0.05 was considered statistically significant

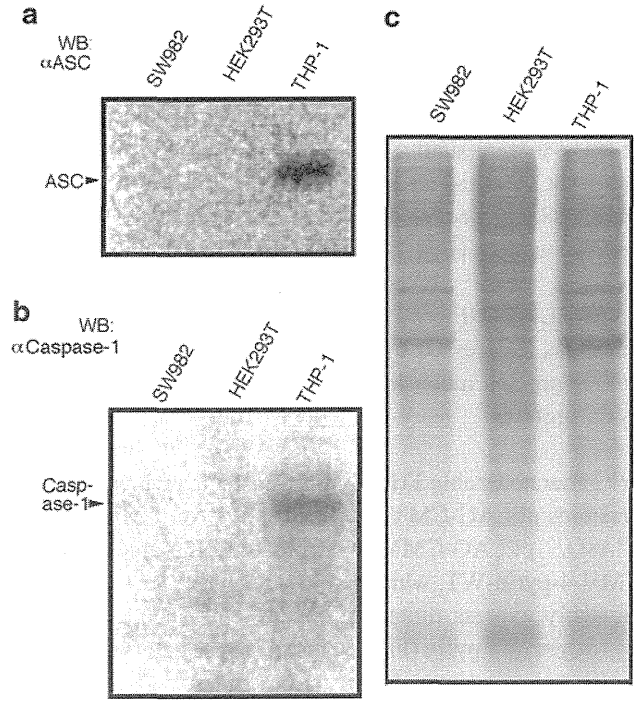

Fig. 3 Expression of ASC and caspase-1 in THP-1 cells, SW982 cells, and HEK293T cells by Western blotting analysis. Thirty μg of whole cell lysates of THP-1 cells, SW982 cells, and HEK293 cells was subjected to Western blotting. **a** Blotting membranes were detected using mouse anti-human ASC monoclonal antibody [26]. **b** Blotting membranes were detected using rabbit anti-human caspase-1 polyclonal antibody (Cell Signaling Technology, Danvers, MA, USA). **c** Gel was stained with Coomassie Brilliant Blue

1β, IL-6, IL-8, or TNF-α with 10 ng/ml LPS stimulation (Fig. 4a); for IL-1β, IL-8, and TNF-α, each cytokine secretion was significantly suppressed by WT pyrin but suppressed much less by M694V pyrin (Fig. 4a, b). In terms of IL-6 secretion from THP-1 cells, there was no significant difference among all the mutations (Fig. 4a, b).

Pyrin affects ERK1/2 phosphorylation of SW982 cells

We found that p38 and ERK 1/2 were spontaneously phosphorylated even when mutated M694V and E148Q pyrin proteins were ectopically expressed in SW982 cells (Fig. 5a, b). ERK1/2 was found to be less phosphorylated when WT pyrin was ectopically expressed in SW982 cells (Fig. 5b). On the other hand, there was no significant phosphorylation in NF-κB p65 for NF-κB activation (Fig. 5c).

Peripheral blood mononuclear cells from FMF patients secreted IL-8 when incubated on a culture plate

We obtained peripheral blood mononuclear cells from five FMF patients with *MEFV* mutations; four patients were

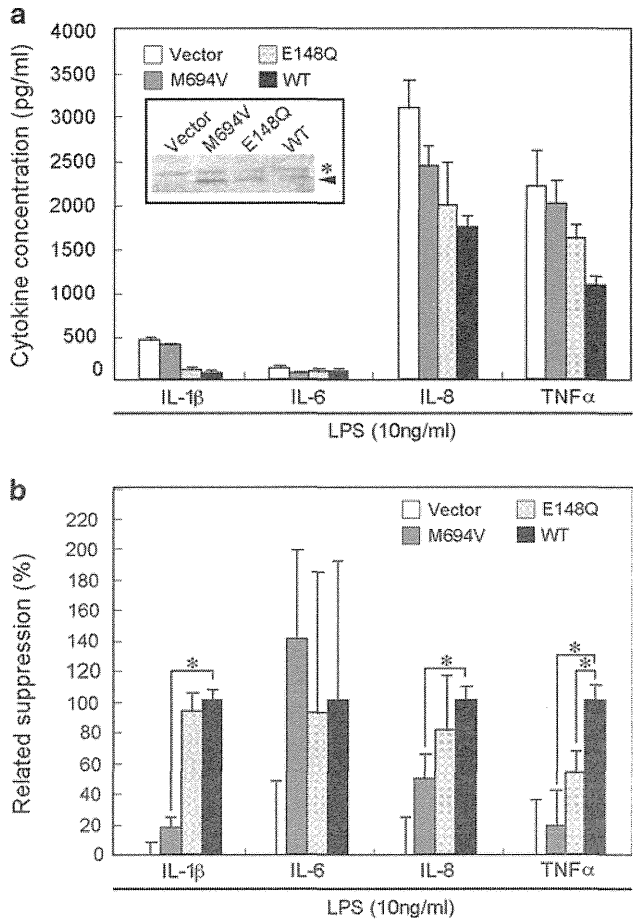

Fig. 4 Interleukin 1β, interleukin-6, interleukin-8, and TNF-α secretion from stable THP-1 cells. **a** 1×10^7 monocytic leukemia THP-1 cells were transfected with 5 μg of pFLAG-CMV-4 (Vector), pFLAG-CMV-4-pyrin-WT, pFLAG-CMV-4-pyrin-E148Q, or pFLAG-CMV-4-pyrin-M694V. After incubation with 500 μg/ml G418 (Sigma) in RPMI 1640 medium including 10 % FBS for 4 weeks to generate stable THP-1 cells. Wild-type (WT) and mutated pyrin expressions were confirmed by Western blotting (*inset*, *arrowhead*; *asterisk* is non-specific band). THP-1-derived stable cells expressing WT and mutated pyrin proteins were pre-cultured in 24-well flat-bottomed plates to a final cell density of 2×10^7/ml in a volume of 300 μl of RPMI1640 Medium including 10 % FBS for 8 h at 37 °C in a humidified atmosphere with 5 % CO_2. Then, the culture medium was supplemented with 300 μl of RPMI1640 containing 20 ng/ml LPS. 8 h after medium replacement, the concentrations of IL-1β, IL-6, IL-8, and TNF-α in the culture supernatant were measured by enzyme-linked immunosorbent assay with specific antibodies (BD Biosciences, San Jose, CA, USA). **b** Percentiles of relative suppression of IL-1β, IL-6, IL-8, or TNF-α secretion from THP-1 cells expressing mutated pyrin versus WT pyrin were calculated from triplicate cultures. *A p value <0.05 was considered statistically significant

E148Q/M694I compound heterozygotes and one patient was an E148Q/E148Q homozygote. We found a significant difference between five FMF patients and five healthy volunteers in terms of IL-8 secretion from mononuclear cells, even when incubated on a culture plate for 6 h (Fig. 6a, b). Peripheral blood mononuclear cells from FMF

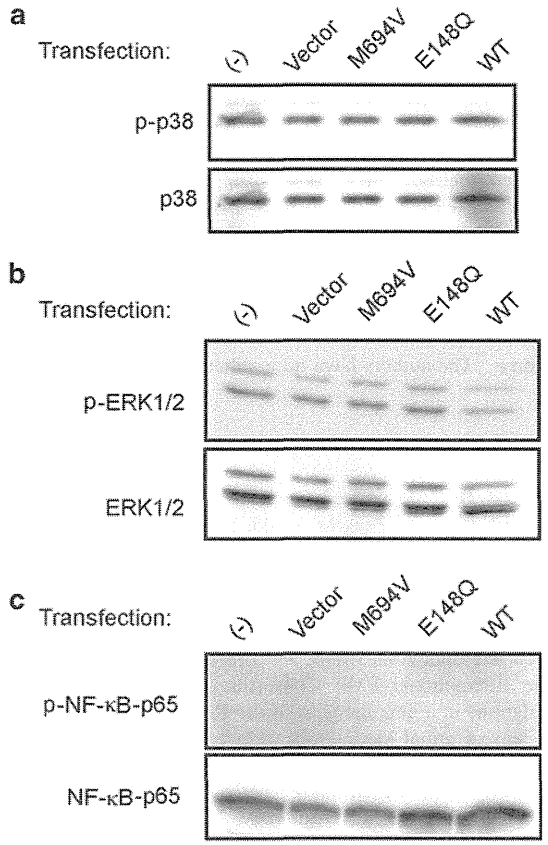

Fig. 5 Western blotting analyses for p38, ERK, and NF-κB pathways. 40 μg of SW982 cell lysates were subjected to SDS-PAGE followed by Western blotting analysis for p38, ERK, and NF-κB pathways. Signals from the same blotting membrane were detected by phospho-p38 MAPK (Thr180/Tyr182) rabbit monoclonal antibody and p38α MAPK rabbit polyclonal antibody for the p38 pathway (**a**), or phospho-p44/42 MAPK (Erk1/2) (Thr202/Tyr204) rabbit monoclonal antibody and p44/42 MAPK (Erk1/2) rabbit monoclonal antibody for the ERK pathway (**b**), or phospho-NF-κB p65 (Ser536) rabbit polyclonal antibody and NF-κB p65 rabbit monoclonal antibodies for the NF-κB pathway (**c**)

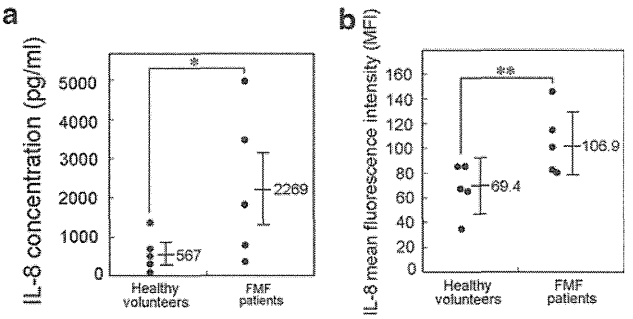

Fig. 6 IL-8 secretion from mononuclear cells from FMF patient with pyrin mutations compared with healthy volunteers. **a** 5×10^5/ml peripheral blood mononuclear cells were incubated in 96-well flat plates with RPMI1640 with 10 % heat-inactivated FBS for 6 h. The supernatants were collected and analyzed for IL-8 concentration (pg/ml) with the Cytometric Bead Array Flex set. **b** 5×10^5/ml mononuclear cells including BD GolgiPlug protein transport inhibitor (BD Biosciences) were incubated under the same conditions as described above. After 6 h of incubation, adherent cells were collected by pipetting. The cells were fixed using a BD Cytofix/Cytoperm solution for 20 min at 4 °C, then fixed cells were permeabilized by washing two times in 1 × BD Perm/Wash buffer. Intracellular IL-8 was stained with FITC-conjugated anti-IL-8 monoclonal antibody and flow cytometric analysis was performed with a FACSCalibur flow cytometer and mean fluorescence intensity (MFI) was calculated. *, ** p values <0.05 and <0.01 were considered statistically significant, respectively

patients were found to exhibit higher IL-8 secretion than those from healthy volunteers (Fig. 6a, b). IL-1β concentrations were at an undetectable level under the same conditions (data not shown).

Discussion

We have investigated the relationship between the main pyrin mutations of FMF patients and the suppression of IL-8 secretion from synovial sarcoma SW982 cells. Pyrin was discovered as a causative gene product of FMF, and E148Q, M694I, and E148Q/M694I mutations of pyrin have been found to be the major mutations of Japanese FMF patients [7, 9]. We constructed mutated-pyrin expression plasmids corresponding to the above mutations (Fig. 1a), and found no apparent difference among WT pyrin and mutated pyrin proteins in terms of expression stability and detergent solubility (Fig. 1b, c). We also found that WT pyrin suppressed IL-8 secretion from SW982 cells, but this was less suppressed by E148Q, M694I, M694V, and E148Q+M694I pyrin in that order, and WT pyrin and mutated pyrin proteins did not affect IL-6 secretion from SW982 cells (Fig. 2). Although it is unusual, compared with normal synovia, for SW982 cells spontaneously to secrete IL-8 without any stimulation, it is likely that a similar model is involved in sterile arthritis, which has been found in FMF patients.

Arthritis is one of the major symptoms of FMF patients [8, 19]. The attacks of FMF arthritis are usually acute inflammatory responses, of which the hallmark in the tissue is self-limiting neutrophil infiltration in synovial stroma [20]. Neutrophils are usually recruited by chemotactic factors such as IL-8, which was shown to be induced by epithelial cells or leukocytes in microbial infection or rheumatoid arthritis [21, 22]. However, sterile inflammation in pleura, peritonea, and synovia, which is common in FMF patients, is thought to occur without any microbial infection or rheumatoid factors [23]. FMF-related sterile inflammation is reported to be triggered by dysregulation of inflammasome, an IL-1β processing platform composed of Nod-like receptor (NLR), ASC, and caspase-1 [24]. It was also reported that NLRC4-inflammasome-related NF-κB activation leads to IL-8 secretion from MEIL-8 cells [12]. The NLRC4-inflammasome-related NF-κB activation